Energy & Buildings 362 (2026) 117496

Contents lists available at ScienceDirect

Energy & Buildings

journal homepage: www.elsevier.com/locate/enb

Uncertainty analysis for variables affecting the whole life carbon performance of nearly zero energy residential building renovation☆

Aurora Bertini [a,b,*], Deepak Amaripadath [c,d], Emilie Gobbo [b], Shady Attia [a]

[a] Sustainable Building Design Lab, Dept. UEE, Faculty of Applied Sciences, Université de Liège, Belgium
[b] Louvain Research Institute for Landscape, Architecture, Built Environment (LAB), Faculty of Architecture, Architectural Engineering, and Urban Planning (LOCI), UCLouvain, Belgium
[c] School of Geographical Sciences and Urban Planning, Arizona State University, Tempe, AZ, USA
[d] Urban Climate Research Center, Arizona State University, Tempe, AZ, USA

ARTICLE INFO

Keywords:
Building retrofit
Whole-life greenhouse gas emissions
Lifecycle cost
Dynamic building performance optimization
Latin Hypercube Sampling
Non-dominated Sorting Genetic Algorithm

ABSTRACT

This study investigates the impact of retrofit strategies on the whole-life greenhouse gas emissions (wLCE) and global cost (GC) for two representative Belgian residential archetypes. Six renovation alternatives combining envelope, system, and renewable energy upgrades are optimized using the Non-dominated Sorting Genetic Algorithm (NSGA-II) within a dynamic simulation framework integrating building energy modelling, life-cycle costing, and life-cycle assessment. Uncertainty analysis (UA) based on Latin Hypercube Sampling assesses the sensitivity of wLCE and GC to future electricity mix scenarios, climate change, energy prices, occupants' behavior, materials' service life and quantities. A clear trade-off emerges: deeper emission reductions entail higher investment and life-cycle costs. The best compromise for both archetypes is the intermediate retrofit using biobased materials (S.01b), while high-performance options (S.02a–S.02b) achieve the lowest wLCE but require substantially higher investment. Environmental payback periods range from 14 to 30 years, confirming retrofit effectiveness in reducing wLCE, whereas economic payback exceeds 50 years due to current energy market conditions and limited carbon taxation. Finally, UA reveals that energy price variability most strongly influences GC, while electricity mix, climate change, and occupants' type have the greatest effect on wLCE. Temperature setpoints, materials service life, and materials quantities strongly impact both indicators. This study highlights the need for revised policy frameworks and stronger financial incentives to improve retrofit financial feasibility and accelerate the transition towards cost-effective, low-carbon building renovations.

1. Introduction

1.1. Study background and literature review

The European building sector accounts for 40% of final energy consumption and 36% of energy-related greenhouse gas (GHG) emissions [27]. Yet, progress towards climate neutrality remains too slow [62], with current emission reductions still falling short of the Renovation Wave target of a 60% reduction by 2030 and climate neutrality by 2050 [25].

A key barrier is the persistently low renovation rate. It remains around 1% per year, with only a small share as deep renovations [16]. As a result, heating and cooling energy use declines insufficiently, still accounting for 50% of European Union (EU) energy consumption [16]. At the same time, the slow electrification of heating and cooling, and limited on-site renewable energy, worsen the issue. This leaves buildings responsible for about half of EU gas consumption [23].

To accelerate this transition, the European Commission launched the

Abbreviations: BC, Base Case; BIM, Building Information Modelling; BPS, Building Performance Simulation; COP, Coefficient Of Performance; CV, Coefficient Of Variation; EPDs, Environmental Product Declarations; EU, European Union; GC, Global Cost; GWP, Global Warming Potential; GHG, Greenhouse Gas; LHS, Latin Hypercube Sampling; LCA, Life-Cycle Assessment; LCC, Life-Cycle Cost; LCIA, Life-Cycle Impact Assessment; MOO, Multi-Objective Optimization; nZEB, Nearly-Zero Energy Building; NSGA-II, Non-Dominated Sorting Genetic Algorithm; UA, Uncertainty Analysis; Wlce, Whole-Life Greenhouse Gas Emissions; ZEB, Zero-Emission Building.

☆ This article is part of a special issue entitled: 'ENB_Ecological Buildings' published in Energy & Buildings.

* Corresponding author at: Building 52. Quartier Polytech 1, Allee de la Decouverte 13A, 4000 Liege, Belgium.
E-mail address: aurora.bertini@uliege.be (A. Bertini).

https://doi.org/10.1016/j.enbuild.2026.117496
Received 30 December 2025; Received in revised form 19 March 2026; Accepted 16 April 2026
Available online 21 April 2026
0378-7788/

Renovation Wave strategy [51], which seeks to double both the rate and the depth of building renovations by 2030, levels considered essential to achieving the EU's emission-reduction goals. In parallel, recent European policy developments marked a paradigm shift from primary energy metrics toward emissions-based performance indicators. The 2024 Energy Performance of Buildings Directive (EPBD) recast replaced the nearly-zero energy building (nZEB) standards with the concept of zero-emission buildings (ZEBs), in order to achieve not only zero or very low energy consumption, but also zero on-site carbon emissions from fossil fuels, and zero or a very low amount of operational GHG emissions. The 2024 EPBD recast also sets operational GHG emissions thresholds for both new-built and retrofit projects, complementing the existing primary energy limits, and progressively incorporates life-cycle global warming potential (GWP) calculations for new buildings [27]. This evolution reflects increasing recognition that operational and embodied emissions must be jointly assessed to avoid that increased embodied energy and emissions associated with materials manufacturing, construction, and renovation stages may potentially offset long-term operational benefits [7,52].

However, a significant regulatory and methodological gap remains, resulting in fragmented EPBD implementation across Member States. This leads to significant variations in the definitions of limit values, GHG emission calculation methods, reference units, floor area definitions, building typologies, and building scope. Furthermore, methodological differences, such as included lifecycle modules, static or dynamic life-cycle assessment (LCA) approaches, and the variety of LCA calculation tools and databases, compromise comparability across countries [65].

For building retrofits, the gaps are larger. First, lifecycle GWP requirements for renovations are absent. Only Norway has refurbishment requirements. Sweden, Finland, the Czech Republic, and Switzerland plan to adopt them [65]. Given that 85% of EU buildings were constructed before 2000 and 75% still perform poorly in energy terms [23], the lack of renovation requirements represents a major regulatory gap. Extending wLCE calculations and establishing GHG emission thresholds for retrofits at the level of new buildings would encourage retention and upgrade of existing building stock [65], would foster a more structured, integrated approach to renovation, address the trade-off between embodied and operational emissions, and ensure substantial reductions in buildings' life-cycle emissions.

Second, although EPBD 2024 requires accessible renovation financing, financial uncertainty remains a key obstacle. High investment costs, complex administrative procedures, and unclear funding still discourage households from undertaking deep renovation works [24]. Therefore, even with stronger environmental targets, progress depends on linking climate goals with clear economic evaluations and solid financial support.

Addressing these gaps requires holistic frameworks capable of jointly assessing energy, emissions, and economic performance across the whole-life cycle of retrofit interventions. Such an approach would enable policymakers to identify the most effective renovation pathways and design financial mechanisms to support retrofit investments, while allowing designers and homeowners to prioritize interventions that maximize performance improvements and balance upfront costs with long-term life-cycle savings and environmental benefits. However, this approach remains underexplored.

In published research, few studies have fully integrated Building Performance Simulation (BPS), LCA, and life-cycle cost (LCC) into retrofit optimization (Fig. 1). Al-Kabaha et al. [1] optimized energy consumption, global cost (GC), and operational emissions for a single-family house, focusing on envelope and systems retrofit, while Wen et al. [63] included also renewables in exploring the trade-off between operational emissions and GC. Shan et al. [54] proposed an integrated artificial intelligence framework that accounts for energy, costs, and emissions from manufacturing, shipping, and operational energy use. Dehghan & Porras Amores [20] further expanded the research objectives, aiming to optimize envelope and systems retrofits across different climate scenarios to minimize primary energy use, operational GHG emissions, predicted percentage of dissatisfied, and visual discomfort hours, while improving indoor air quality.

However, integrating BPS, LCA, and LCC poses both methodological and computational challenges. The complexity of reality and the buildings' long service life introduces sources of uncertainty, including: parameters uncertainty (e.g., imprecise measurements, assumptions or estimations of a parameter value), models uncertainty (e.g., assumptions and simplifications of the real world), design uncertainty (e.g., design variations that can occur during the design and construction process), and scenario uncertainty (i.e., uncertainty that arise during the building lifetime, such as occupant behavior, comfort preferences, energy mix evolution, climate change, cost escalation, carbon pricing) [30]. Uncertainties in one domain often propagate to others: for instance, materials' service life affects both cost and emissions, while changes in the future energy mix influence both operational and embodied emissions of construction products [55]. Hence, an integrated uncertainty analysis is essential to yield reliable, policy-relevant outcomes. Such analysis was performed by Felicioni et al. [28], who combined embodied emissions and cost in a building information modelling (BIM) environment under cradle-to-grave boundaries, introducing uncertainty on the discount rate and building service life. H. Zhang et al. [67] focused on occupant behavior and building envelope uncertainties (e.g., airtightness, glazing type, insulation thickness) to identify optimal retrofit solutions for energy efficiency and thermal comfort. Luo et al. [39] investigated the energy–emissions–cost (investment and operational energy) envelope retrofit, comparing different modelling approaches to assess model-prediction uncertainty.

Despite these advances, no study to date has conducted a comprehensive analysis that simultaneously: (i) integrates dynamic whole-life-

	Modelling scope				Ojective function						Modelling approach	Uncertainty analysis	
	Envelope	Structure	Systems	Renewables	Energy	Embodied emissions	Operational emissions	Cost	Visual comfort	Thermal comfort	Static/ Dynamic		
Shan al. (2025)					✓	✓	✓				S		
Felicioni et al. (2025)		✓									S		
Dehghan & Porras Amores (2025)	✓		✓		✓		✓		✓	✓	S	✓	Climate
Al-Kabaha al. (2025)	✓		✓		✓		✓	✓			S		
Wen et al. (2025)	✓		✓	✓			✓	✓			S		
Luo et al. (2025)	✓				✓	✓	✓	✓			S	✓	Model prediction
Zhang et al. (2025)	✓		✓		✓					✓	S	✓	Occupant's behavior Building construction

Fig. 1. Literature review contributions to multi-objective optimization and uncertainty analysis in building retrofit.

cycle assessment and LCC optimization for building retrofits; (ii) covers as wide a scope as the building envelope, building systems, and on-site renewables; (iii) accounts for variability in whole-life GHG emissions (wLCE) and global cost (GC) results within the framework through uncertainty analysis (UA).

The present study addresses this gap and applies an integrated assessment framework to: (i) investigate the trade-off between wLCE and GC in residential building retrofit strategies, and identify the cost-optimal renovation solutions that combine active and passive strategies to achieve net-zero-carbon buildings; and (ii) evaluate to what extent the residential building archetype, climatic and future energy scenarios, occupants' behavior, and uncertainties in materials service life and quantity impact the choice of dwelling renovation strategy.

1.2. Study relevance and research objectives

To address the identified research questions, six renovation alternatives are evaluated for two Belgian single-family house archetypes. These alternatives focus on the building envelope, technical systems, and on-site renewable integration. A multi-objective optimization (MOO) is conducted to identify optimal retrofit solutions in terms of wLCE and GC. In parallel, UA assesses the variability of wLCE and GC across different climate scenarios, electricity mix, and energy price projections, as well as uncertainties related to occupants' behavior, materials' service life, and materials quantities.

Integrating dynamic whole-life cycle assessment and dynamic LCC into both MOO and UA represents the main novelty of this study. The research performs a whole-life-cycle calculation for emissions and cost, encompassing stages A0-A5, B4, B6, and C4 for the economic assessment [11]. the Danish approach guides stage selection (A1-A5, B6, C3-C4). The analysis encompasses a comprehensive renovation scope, including the envelope, systems, and on-site renewable energy technologies while accounting for finishes' contributions to emissions and costs. Building geometry variability is addressed through two single-family houses archetypes; these share envelope and system performance but differ in geometric configurations.

The study also adopts a dynamic calculation approach to capture the evolution of energy prices and carbon taxation. Future climatic conditions and energy mixes are also modelled dynamically. Their joint influence on wLCE and GC is assessed within the UA, along with cost variations, occupants' behavior, materials' service life and quantities. By assessing both economic and environmental indicators, the UA goes beyond the energy indicator alone. This allows explicit, policy-oriented interpretation of the results. Finally, the study includes a detailed MOO Pareto post-processing procedure to identify the most suitable and balanced retrofit strategies.

The paper is structured as follows: Section 1 situates the research within the European context and reviews the literature on MOO and UA in building retrofit. In Section 2, the adopted methodology is described, presenting the case study and the renovation alternatives, the modelling

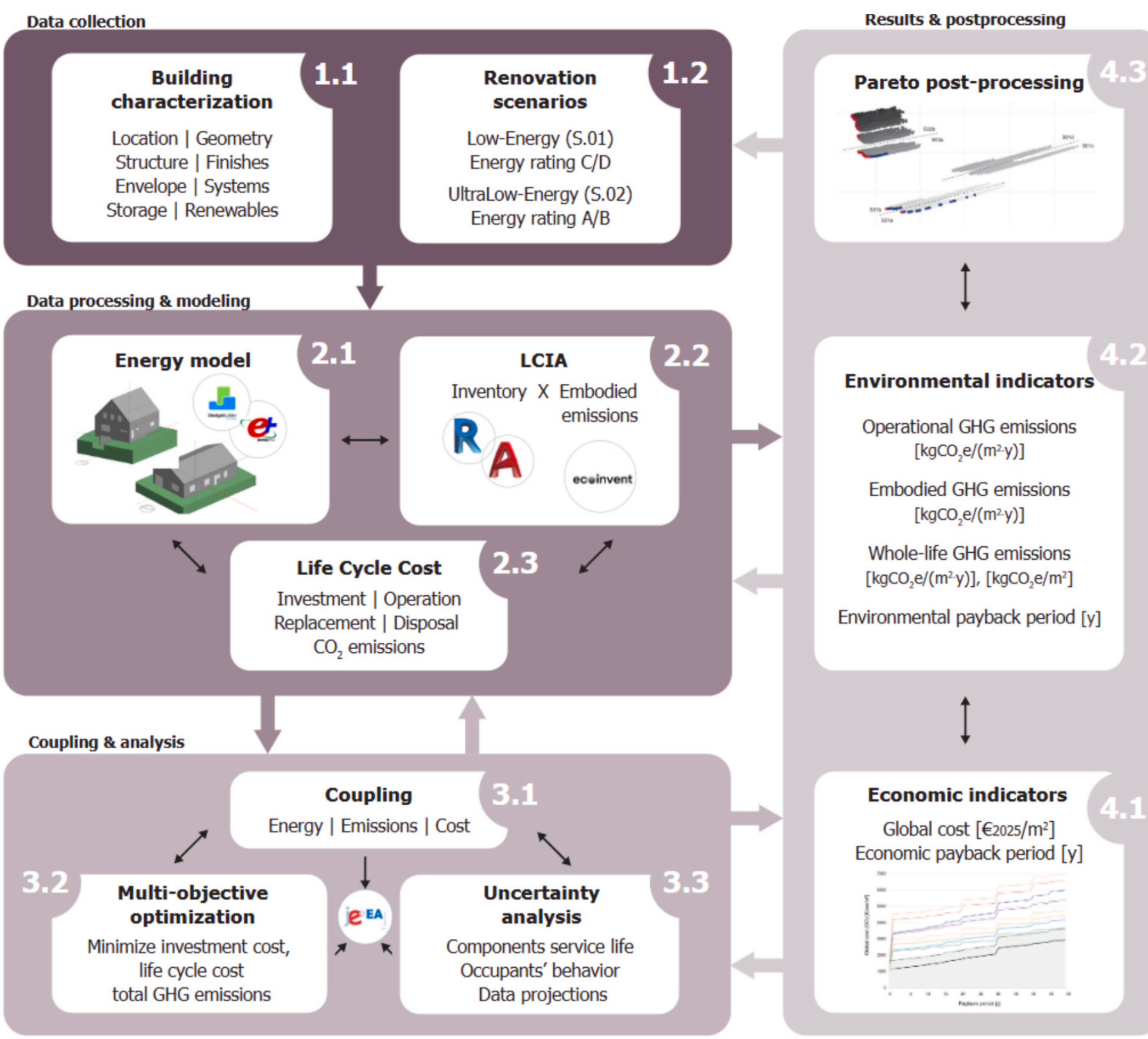

Fig. 2. Study conceptual framework.

approaches for energy, emissions, and cost calculations, as well as the MOO and UA techniques. Section 3 presents the results, beginning with MOO outcomes and Pareto post-processing, followed by an assessment of the impact of uncertainty. In Section 4, the findings are discussed; key insights, strengths, and limitations of the study are highlighted, and recommendations for future research are provided. Section 5 concludes the manuscript.

2. Methodology

Fig. 2 illustrates the adopted methodology. Following the characterization of the location and the case study buildings (Archetypes A and B), two renovation scenarios were developed for each: a Low-Energy scenario (S.01), targeting energy class C/D, and an UltraLow-Energy scenario (S.02), targeting class A/B. Each scenario incorporated two material options (petrochemical and biobased). In S.01, two mechanical ventilation systems (C and D) were tested, yielding a total of six renovation alternatives.

For each alternative, environmental and cost data were collected. Embodied GHG emissions were assessed over 50 years in accordance with EN 15804 + A2:2019 [14] and EN 15978 [11], using material inventories from Revit and AutoCAD and impact data from TOTEM [60] (integrating Ecoinvent). Operational emissions were calculated using country-specific electricity mix data from ElectricityMaps [22]. GC, determined in accordance with EN 16627 [12], included investment, replacement, disposal, and operational costs, with values adapted to the Belgian context.

Energy models were developed in DesignBuilder v7.3.0 [21]. Next, the exported.idf files were modified in jE+EA [68] to integrate cost data and enable GC and investment cost calculations. Outputs were further customized to calculate operational emissions, which were combined with embodied emissions resulting from the lifecycle impact assessment (LCIA) to obtain total GHG emissions for each scenario and parameter combination. The indicators total GHG emissions, GC, and investment cost were employed in a multi-objective optimization, minimizing all three simultaneously. Uncertainty analysis assessed their sensitivity to selected parameters. Finally, optimization results were post-processed in Python to perform Pareto analysis and calculate economic and environmental payback periods.

The analysis was conducted under fixed boundary conditions: a one-stage renovation at the beginning of the study reference period; solutions reflecting both market feasibility and future technological potentials, combining conventional and advanced retrofit measures; application of all renovation scenarios to both archetypes without design modification; exclusion of gas boilers in compliance with existing policies [26]; and omission of construction-phase energy use and scaffolding costs from the economic analysis. This last assumption may lead to an underestimation of life-cycle costs, particularly in deep renovation scenarios, since such interventions require more extensive site activities and longer construction periods. Consequently, the results may favor envelope-intensive retrofit strategies by failing to fully account for their associated economic burdens. However, it is not expected to change the ranking of retrofit strategies, only the absolute results, since deep retrofits are expected to be significantly more expensive than intermediate retrofits.

2.1. Data collection

2.1.1. Building characterization

The study focuses on the Belgian context, selected for the relevance of existing case studies [5] and the possibility to examine the impact of future changes in the national electricity mix, particularly in light of the planned temporary phase-out of nuclear power [49].

Two post–World War II Belgian single-family houses archetypes were analyzed: Archetype A, representing dwellings built between 1945 and 1969, and Archetype B, representing those built between 1970 and 1990. These together account for 48% of the existing Belgian building stock [5]. A detailed description of the archetypes is provided by Attia et al. [5].

Both archetypes are set in Brussels, Climate Zone 4A [3], and are occupied by seniors. Archetype A typically houses occupants over 70, in couples or single female seniors. Archetype B residents are generally over 60 and include at least one retired person.

The two archetypes differ primarily in geometry. Archetype A has a larger gross floor area (235 m^2, excluding attic and garage) and a split-level layout: garage at level − 1, living area at level 0, bedrooms at level + 1, and an attic at level + 2. Archetype B is smaller (152 m^2) and organized entirely on a single level, supplemented by an attic.

From a construction standpoint, both have a load-bearing wall structure with cavity walls clad in brick. Archetype A features a cast concrete garage floor and hourdi concrete block floors elsewhere, whereas Archetype B uses prefabricated concrete slabs. In both archetypes, the roof structure is timber, finished with fired clay tiles. The ground floors are finished with clay tiles, while the upper levels use timber flooring.

Envelope and system performance are comparable (Appendix A – Table A1) and reflect partial renovations before 2000: ground floor and roof insulation, double glazing, and shading devices. Heating and domestic hot water (DHW) are supplied by gas boilers; no cooling or mechanical ventilation systems are present.

Despite these upgrades, Archetype A exhibits an annual energy use intensity of 166 kWh/(m^2·y): 148.7 kWh/(m^2·y) for heating and DHW, 17.7 kWh/(m^2·y) for electricity. This corresponds to energy class F and operational GHG emission intensity of 32 $kgCO_2e/(m^2·y)$. Archetype B achieves energy class E with an annual energy use intensity of 155 kWh/(m^2·y) (139.8 kWh/(m^2·y) for heating and DHW, 14.9 kWh/(m^2·y) for electricity), resulting in annual operational GHG emissions of 33 $kgCO_2e/(m^2·y)$.

2.1.2. Renovation scenarios

Retrofit covers the building envelope, technical systems, and on-site renewables. To reflect market reality while testing advanced, optimal retrofit solutions, two retrofit scenarios were designed: Low-Energy (S.01), targeting energy class C/D, and UltraLow-Energy (S.02), targeting class A/B.

S.01 represents an intermediate performance level between the non-retrofitted base case (BC) and S.02. It relies on more affordable but less efficient solutions. In contrast, S.02 adopts high-performance materials and technologies. Accordingly, S.01 includes two mechanical ventilation variants, type C (S.01a) and type D (S.01c), whereas in S.02 only Type D is considered (S.02a). In addition, each scenario compares petrochemical and biobased envelope materials, resulting in variants S.01b, S.01d, and S.02b.

In both alternatives, envelope retrofits target the roof, external walls, windows, and doors. Special attention is given to improving airtightness. Envelope performance requirements in S.02 align with the Passivhaus standard [46], while S.01 aims to achieve an intermediate level between the BC and S.02. These targets affect both insulation thickness and glazing selection. For instance, double glazing is used in S.01, while triple glazing is used in S.02.

Systems upgrades include a reversible air-to-water heat pump with integrated water storage. In S.01, the heat pump delivers 55 °C water to existing radiators. In S.02, floor heating and cooling on the ground floor and low-temperature radiators on Archetype A's first floor allow supply at 35 °C. Both scenarios integrate photovoltaic (PV) panels on the South-West roof pitch. S.01 includes 12 m^2 of polycrystalline PV panels, which are more cost- and environmentally effective but less efficient. In contrast, S.02 includes 32 m^2 of more efficient monocrystalline PVs and 5 m^2 of solar thermal panels to further reduce the heat pump electricity use. PVs are paired with a 5kWh storage battery in S.01, increased to 10kWh in S.02 to match the greater PV surface.

A detailed characterization of all retrofit measures is provided in

Table A1 (Appendix A) and further described in Bertini et al. [7]. Since the BC condition is comparable for both archetypes, identical retrofit scenarios are applied to both, enabling direct performance comparisons across building typologies.

2.2. Data processing and modelling

2.2.1. Energy model

Energy models for renovation scenarios were developed using DesignBuilder 7.3.0 [21], which operates on the EnergyPlus 9.4.0 simulation engine. These models were based on the BC models from Attia et al. [5], calibrated with weather data spanning 2016 to 2019 [5].

The modelling assumptions for Archetype A, summarized in Appendix A (Table A1), follow those established by Bertini et al. [7]. They include distinct occupancy, heating, ventilation, and lighting schedules, as well as temperature setpoints for each zone (living areas, sleeping areas, and short presence spaces). Heating operates from October to April, cooling from May to September, and mechanical ventilation runs 24/7. In scenarios with ventilation system D, mixed mode allows natural ventilation when external temperature conditions are adequate and cooling is not required. These assumptions were adapted as required to accurately represent Archetype B, mainly by modifying occupancy and heating schedules, and heating temperature setpoints to reflect differing occupant profiles.

The sole deviation from the original methodology is the integration of a battery system to store surplus PV generation prior to exporting excess electricity to the grid [2]. Battery and inverter specifications were sourced from manufacturers' datasheets.

2.2.2. Life cycle impact assessment (LCIA)

An attributional LCIA approach was adopted in accordance with EN 15804 + A2:2019 [14] and EN 15978 [11]. As for the energy modelling, the LCIA methodology aligns with that described in Bertini et al. [7].

Calculations were performed over a 50-year reference period. This aligns with the default value commonly adopted for new buildings in life cycle assessment (LCA) studies. In addition to this widely used approach, Decorte et al. [19] identified two alternatives. The first option defines the reference period as the difference between the building's age and its total service life. However, assuming a total service life of 100 years, this approach would yield different reference periods for the two selected archetypes: 20 to 44 years for the older building, and 45 to 65 years for the more recent one. Such situation would complicate comparisons across archetypes. The second option sets the study reference period to the calculated service life extension resulting from renovation. Yet, no guidelines currently support this method. Implementation would require adapting default values to account for current building conditions, renovation depth, maintenance levels, and environmental factors. Each archetype also represents a large number of real buildings, making this approach difficult to implement, as it would require assumptions about building-specific conditions. For these reasons, a uniform 50-year study reference period was adopted to make archetypes easier to compare and align with major LCA practices.

Environmental data were sourced from TOTEM [60], the Belgian benchmark tool that integrates Ecoinvent [64] for calculating the environmental impact of buildings. TOTEM was used for product- and component-specific impact data. Verified Environmental Product Declarations (EPDs) were prioritized. Secondary data from Ecoinvent were used when necessary. For the materials inventory, data on structural, architectural, and envelope components were extracted from Revit models. Mechanical systems, such as ventilation ducts and connections, were modeled in AutoCAD. Systems' material quantities were manually quantified based on technical sheets, CIBSE TM65 guidelines [15], and EPDs for critical components such as steel, aluminum, and plastics. Calculations covered Modules A1–A3, A4–A5, B4, and C3–C4 (Table 1), following EN 15804 + A2 guidelines [14], with data regionalized for Belgium. Brightway2, an open-source LCA framework, allowed

Table 1
Life cycle stages included in the environmental and economic assessments (adapted from EN 16627).

	Pre-Construction (A0)	Product (A1 – A3)			Construction (A4 – A5)		Use (B1 – B7)							End of Life (C1 – C4)				Beyond the Building Life-Cycle (D)
	A0. Land and associated fess/advice	A1. Raw materials extraction	A2. Transport	A3. Manufacturing	A4. Transport	A5. Construction	B1. Use	B2. Maintenance	B3. Repair	B4. Replacement	B5. Refurbishment	B6. Operational energy use	B7. Operational water use	C1. Deconstruction	C2. Transport	C3. Waste processing	C4. Disposal	Reuse / Recovery / Recycling potential
Environmental assessment		✓	✓	✓	✓	✓				✓		✓				✓	✓	
Economic assessment	✓	✓	✓	✓		✓		✓		✓		✓					✓	

advanced, customizable LCA modeling in Python. This provided flexibility for defining system boundaries and impact assessment methods. The LCIA of building services, including heat pumps, PV panels, ventilation ducts, AHUs, and heat recovery units, was conducted using the Building Carbon Modeling Framework [6].

The only variation proposed to this methodology is the different allocation of PV panel emissions. In Bertini et al. [7], PV emissions were fully allocated to the building. In this study, instead, PV emissions are shared with the grid according to the amount of energy that is exported to the grid [34]. In fact, this choice is meant to reduce the embodied emissions "penalty" on the houseowner. However, it must be noted that the model does not account for the effect of this methodological choice on the emission factor, nor the consequences of on-site generation on the electricity mix.

2.2.3. Life cycle cost (LCC)

According to EN 16627 [12], the economic assessment covers both the building and its site over a 50-year reference study period, consistent with the LCIA. The life-cycle stages included are: A0 (purchase of existing building), A1–A3 (product manufacturing), A5 (renovation works and professional fees), which together form the investment costs; B2 (maintenance), B4 (component replacement), and B6 (operational energy costs and renewable generation revenues), that make up the operation costs; and C4 (material disposal) (Table 1). Given these inclusions, the present analysis qualifies as life cycle costing in accordance with ISO 15686–5 [31]. The adopted macroeconomic approach [10] includes the cost of emissions from primary energy and excludes VAT and subsidies.

For investment costs, building purchase values were derived from COZEB3 and adjusted for partial prior renovations (Section 2.1.1) and market data. Because detailed Belgian data on renovation materials and labor were missing, renovation costs were based on Italian price lists [50] and adapted for Belgium using Association Belge des Experts [4] data and inflation rates (4.4% in 2024; 2.9% in 2025). Heat pump costs were sourced from Olympios et al. [45] and adjusted to the Belgian context. A comprehensive breakdown of the investment cost calculations is summarized in Appendix A (Table A2). The final estimates align with Belgian market benchmarks of about 1,500$€_{2025}/m^2$ for average and 2,500$€_{2025}/m^2$ for high-quality renovations [37,43,48].

Operation costs were actualized with a discount rate of 3%/y to balance initial cost solutions and annual operating costs [10,12].

Energy prices (0.086$€_{2025}$/kWh for gas, 0.298$€_{2025}$/kWh for electricity, 0.060$€_{2025}$/kWh for feed-in) were sourced from DareToCompare. be [17]. Following the COZEB3 methodology, short-term price peaks linked to geopolitical crises were excluded, and prices were projected using a discount rate of 1.81%/year [10].

Maintenance costs followed EN 15459–1 [13], while replacement costs were based on EN 15459–1 [13], COZEB2 [38], and TOTEM [60] service lives. A 3.5%/year price development rate was used [41]. For components with a lifespan exceeding the 50-year reference period, residual investment values were calculated. Table 2 presents a selection of service life values.

Disposal costs were adapted from Regione Lombardia [50] using the same methodology as for investment cost adaptation. They were calculated by material type and based on weight. Finally, CO_2 emissions costs were computed using the carbon pricing values from COZEB3. Consistent with EN 16627, the cost is based on primary energy consumption, calculated by multiplying electricity by 2.5 and natural gas by 1 [29].

Table 2
Materials service lives introduced in the uncertainty analysis.

Material	Minimum SL	Average SL	Maximum SL
Finishes			
Cladding	40	50	60
Internal painting	8	10	12
Envelope			
ETICS/Biobased insulation	40	50	60
Windows	25	30	35
External doors	25	30	35
Systems			
Heat pump	15	20	25
Fancoil	12	15	20
Mechanical ventilation (C/D)	12	15	20
PV panel	15	20	25
Solar panel	15	20	25
Storage systems			
Heat pump water tank	15	20	25
Solar thermal water tank	15	20	25
Battery (5/10 kWh)	5	10	15

2.3. Coupling and analysis

2.3.1. Coupling

Energy, emissions, and cost models were integrated within the jE+EA [68] environment, the platform used for multi-objective optimization and uncertainty analysis. Each renovation scenario was represented by an EnergyPlus (.idf) file exported from DesignBuilder (Section 2.2.1), which served as the baseline energy model in jE+EA. These input files were then modified in jE + EA to incorporate cost-related data directly or, where parameter ranges were required (Section 2.1.2, Appendix A – Table A1), by linking to a Python script.

Through jE+EA's customizable output functions, additional cost components derived from energy simulation results (e.g., CO_2 emissions costs and energy costs) were integrated into the LCC calculation. Similarly, embodied emissions, calculated separately via Python for each renovation scenario, were combined with operational emissions from the simulations to obtain total GHG emission intensity (wLCE).

This workflow enabled simultaneous computation of energy performance, GC, and wLCE for each renovation scenario, ensuring consistent, comparable outputs across all metrics (Sections 2.4.1 and 2.4.2).

2.3.2. Multi-objective optimization

The multi-objective optimization was conducted in jE+EA. The simulation utilized the following inputs: the modified.idf file of each renovation scenario integrating cost, emissions and energy calculations (Section 2.3.1); the weather file for recent climate conditions (2016–2019), to which the model was calibrated (Section 2.2.1); and parameter ranges for envelope, systems, and on-site renewables to be optimized (Appendix A – Table A1). These key parameters, identified in Bertini et al. [7], include external wall, roof, ground floor, glazing and door thermal transmittance, glazing g-value, airtightness, heat pump COP, and PV panels efficiency.

For both Archetypes and each renovation scenario, three conflicting objective functions were identified: wLCE, GC, and the initial renovation investment (CAPEX). As a result, two Pareto fronts, i.e., sets of non-dominated solutions, were identified: wLCE-GC and wLCE-CAPEX.

Simulations were performed for each renovation scenario separately. Results were then gathered to identify the Pareto fronts and the optimal solutions across all available scenarios for each Archetype.

The Non-dominated Sorting Genetic Algorithm 2 (NSGA-II) exploration strategy [18] was adopted. This methodology is widely applied in building design and renovation optimization [40,66], as it provides greater accuracy, better convergence near the true Pareto-optimal [18], and rapid identification of optimal solutions compared with other multi-objective evolutionary algorithms [66].

Considering the model complexity and to achieve a compromise between accuracy and computational time, an initial sample size of 50 was chosen, with 50 new solutions per generation, a 100% crossover probability, a 40% mutation rate, and a maximum of 200 generations per renovation scenario. This configuration enabled the exploration of approximately 9000 solutions per scenario.

Six renovation scenarios were evaluated for each archetype, totaling

1200 generations and about 54,000 solutions per archetype. Archetype A's model is more complex, with more thermal zones than Archetype B. As a result, the average computational time per generation was about 3.0 min for Archetype A and 2.2 min for Archetype B. Overall, the total computation time was about 60 h for Archetype A and 45 h for Archetype B.

2.3.3. Uncertainty analysis

UA was based on a Latin Hypercube Sampling (LHS) exploration strategy [57]. LHS is a Monte Carlo sampling method and is the most popular exploration strategy in UA, requiring a smaller sample than other exploration strategies to achieve the same accuracy [42]. In this study, a sample size of 600 was sufficient to ensure convergence (i.e., variation in the mean and standard deviation lower than 1%).

The analysis quantified the impact of uncertainties in electricity mix projections, climate change scenarios, energy price evolution, occupants' behavior, materials' service life, and material quantities on wLCE and GC.

For the electricity mix, a static scenario with a fixed electricity mix was compared with a dynamic scenario reflecting projected changes in the Belgian electricity mix up to 2050. The static scenario was based on the current electricity mix, which is dominated by nuclear power. Natural gas and renewable sources, mainly wind and solar, are the next largest contributors. This mix results in an annual average emission factor of 0.174 kgCO_2e/kWh. In contrast, the dynamic scenario captures the effects of nuclear plant shutdowns under a business-as-usual scenario consistent with RCP 8.5 projections [49]. In this scenario, natural gas compensates for the phase-out of nuclear energy, while renewable energy penetration remains limited. As a result, the emission factor doubles compared to current levels, reaching 0.325, 0.345, and 0.312 kgCO_2e/kWh in 2030, 2040, and 2050, respectively. Data for the current electricity mix were obtained from Electricity Maps [22]. Future electricity mix and corresponding emission factors were sourced from Ramon & Allacker [49] and Bertini et al. [7].

To assess climate change effects, a static scenario assuming constant energy use over the building life was compared with a dynamic scenario based on RCP 8.5 projections up to 2070. Future decadal weather files were generated using Meteonorm [44].

Regarding energy prices, data were sourced from Brinkhaus [9], which considers three scenarios: Central, Tensions, and GoHydrogen. The Central scenario aligns with the European policy goals to minimize dependence on fossil fuel imports. Tensions reflects intensified geopolitical crises, greater societal tensions, a rise in political parties opposing a rapid, clean energy transition, and shortages of skilled workers. These factors slow renewable expansion. GoHydrogen envisions a comprehensive transformation of the energy system towards climate neutrality by 2050. In this scenario, hydrogen becomes a major energy carrier, and electrification advances rapidly across sectors.

For occupants' behavior, uncertainty in heating and cooling setpoints was analyzed. Heating temperatures ranged from 18 to 23 °C, and cooling setpoints from 25 to 27 °C. These values were based on ISO17772-2 [32] and were adjusted for occupant age and their thermal sensitivity [61]. Heating and cooling setpoints were varied simultaneously, as the interaction risk was minimal due to low cooling energy use. Additionally, the calibrated senior occupant model was compared with a young family of four (two adults and two children) by adjusting occupancy patterns, HVAC schedules, and appliance power and usage per ISO 18523–2 [33].

Variations in the average service life for finishes, wall insulation, windows, doors, and systems were determined based on TOTEM [60] and EN 15459–1 [13] (Table 2).

Finally, material quantities were varied by ± 10% to account for project or construction differences [7].

2.4. Results and post-processing

2.4.1. Economic indicators

Three main economic indicators were considered: initial investment cost, global cost, and payback period.

The initial investment cost (expressed in €$_{2025}$/m2) includes the house purchase, renovation costs, and associated professional fees (stages A0-A5, Section 2.2.3). This cost was normalized by the gross floor area.

According to EN 15459–2 [13], the global cost (*GC*), expressed in €$_{2025}$/m^2, is the sum of several elements. It includes the initial investment cost (CO_{init}) and actualized operation costs (CO_a), such as maintenance, replacements for each component or service (*j*) and operational energy costs (Section 2.2.3). It also covers annual CO_2 emissions costs (CO_{CO2}) over the study reference period (*TC*), and disposal costs at the end of each component's service life ($CO_{f(TLS)}$). Residual values ($VAL_{f(TC)}$), as shown in Equation (1), are subtracted. The global cost was normalized by the gross floor area (*GFA*) (Section 2.1.1).

$$GC = \frac{CO_{INIT} + \sum_J [\sum_{i=1}^{TC} (CO_{a(i)}(j) \bullet (1 + RAT_{(i)}(j)) + CO_{CO2(i)}(j)) \bullet Df_{(i)} + CO_{f(TLS)}(j) - VAL_{f(TC)}(j)]}{GFA} \quad (1)$$

The payback period is the time required to recover the renovation investment cost relative to the non-renovated BC. It is expressed in years and calculated as follows (Equation (2)) [13]:

$$\sum_{i=1}^{TPB} CF_i \bullet \left(\frac{1}{1 + RAT_{(i)}}\right)^t - CO_{INIT} + CO_{INIT,\,ref} = 0 \quad (2)$$

CF_t is the cashflow difference (i.e., the difference of annual costs between the renovation scenarios and the non-renovated BC scenario in the year *i*). *TPB* is the last year for the payback period (i.e., the year when the formula becomes negative or equal to zero). $CO_{init,ref}$ is the initial investment cost of the BC, which is the house purchase.

2.4.2. Environmental indicators

Annual operational emissions include the building's net energy used (OE_{energy}) and refrigerant leakage from the heat pump (OE_{ref}), normalized by the gross floor area. They were calculated according to Equation (3)[6]:

$$OE = OE_{energy} + OE_{ref} = (Annual\,Net\,Energy\,Use \bullet EF) + (G \bullet \omega \bullet \alpha) \quad (3)$$

Annual operational emissions from energy use were calculated by multiplying the annual net energy use intensity (kWh/(m^2.y)) by the annual emission factor (*EF*, kgCO_2e/kWh) of the electricity mix. The annual net energy use intensity accounts for energy used for heating, cooling, mechanical ventilation, domestic hot water, lighting, and equipment, and subtracts electricity produced on-site by PV panels. The emission factor, sourced from Electricity Maps [22], is equal to 0.174 kgCO_2e/kWh.

Refrigerant emissions were calculated by multiplying the refrigerant charge (*G*, corresponding to 3.25 kg of R-32), the GWP of the refrigerant (*ω*, equal to 675 kgCO_2e/kg), and the annual leakage (*α*, equal to 5%). This results in 0.55 kgCO_2e/(m$^{2\cdot}$ y) [7].

Operational emissions were combined a posteriori with embodied emissions (Section 2.2.2). This gave the total annual GHG emissions (wLCE) for each renovation scenario and parameter combination.

Similar to the economic payback period, the environmental payback period was calculated to evaluate the time required to offset the renovation's embodied emissions (*EE*) compared to the non-renovated BC. It is expressed in years and calculated according to the following formula (Equation (4)):

$$\sum_{i=1}^{TPB} OE_i - EE + EE_{ref} = 0 \quad (4)$$

2.4.3. Pareto post-processing

In multi-objective problems, there is generally no single best solution that fully satisfies all criteria [47]. Instead, a set of solutions exists in which no solution is strictly better than any other across all objectives. These solutions are referred to as Pareto-optimal solutions or the Pareto front. Pareto post-processing involves analyzing and filtering the Pareto front after it has been generated to obtain a small subset of preferred solutions. This facilitates decision-making and enables the evaluation and interpretation of results obtained from any optimization method. Selecting a single solution from the Pareto-optimal set can be challenging, since in the absence of subjective or judgmental information, no solution is inherently superior to the others [59].

Pruning aims to reduce the size of the Pareto set by applying predefined rules [47]. In this study, a non-numerical pruning method was adopted [58]. In this approach, the objective functions are scaled and then ranked non-numerically by the decision maker [59].

The algorithm was implemented in Python. Since the preferences of the decision makers were unknown, all six possible objective combinations were analyzed: i) GC, wLCE, CAPEX (GEI); ii) GC, CAPEX, wLCE (GIE); iii) wLCE, GC, CAPEX (EGI); iv) wLCE, CAPEX, GC (EIG); v) CAPEX, GC, wLCE (IGE); vi) CAPEX, wLCE, GC (IEG).

3. Results

3.1. Cost-Emissions trade-off and optimal renovation solutions

The BC of Archetype A, representing the existing building prior to renovation, is characterized by a GC of 2800 €$_{2025}$/m^2 and wLCE of 40.5 kgCO_2e/(m$^{2\cdot}$ y) (Fig. 3). All investigated renovation strategies achieve reductions in GHG emissions compared to this baseline. However, these improvements are systematically associated with higher GC and greater upfront investment costs (CAPEX), which become increasingly significant as higher performance levels are targeted. Starting from an investment cost of 1100 €$_{2025}$/m^2 in S.01a, representing 30% of the GC (3630 €/m^2), the share progressively increases in S.01b, reaching its maximum in S.02a and S.02b, with investment cost of 2140 €$_{2025}$/m^2 corresponding to 42% of the GC (5020 €$_{2025}$/m^2) (Appendix A – Table A2).

Strategies S.01c and S.01d are exceptions. Installing a type-D ventilation system increases investment, maintenance, and replacement costs compared to S.01a and S.01b. Despite these costs, it does not achieve meaningful reductions in wLCE because the ventilation system's embodied emissions and additional operational energy use offset any savings. For this reason, both scenarios were excluded from Pareto-optimal solutions.

In terms of GC, S.01a performs best, whereas S.02b incurs the highest costs. Conversely, S.02b achieves the lowest wLCE, while S.01a records the highest emissions. However, even S.02b does not meet the Danish emissions threshold (8.2 kgCO_2e/(m$^{2\cdot}$ y)). The best combination yields a wLCE of 9.46 kgCO_2e/(m$^{2\cdot}$ y), so a further 13.3% reduction is needed to comply. This outcome highlights the need for a systemic approach that targets not only the reduction of building emissions but also those associated with materials manufacturing and electricity generation.

To identify the renovation strategy that guarantees the best compromise between wLCE, GC, and CAPEX, the Pareto frontiers were investigated (Fig. 5). The GC-GHG emissions Pareto frontier includes 95 alternatives: 5 from S.01a (5.3%), 5 from S.01b (5.3%), 34 from S.02a

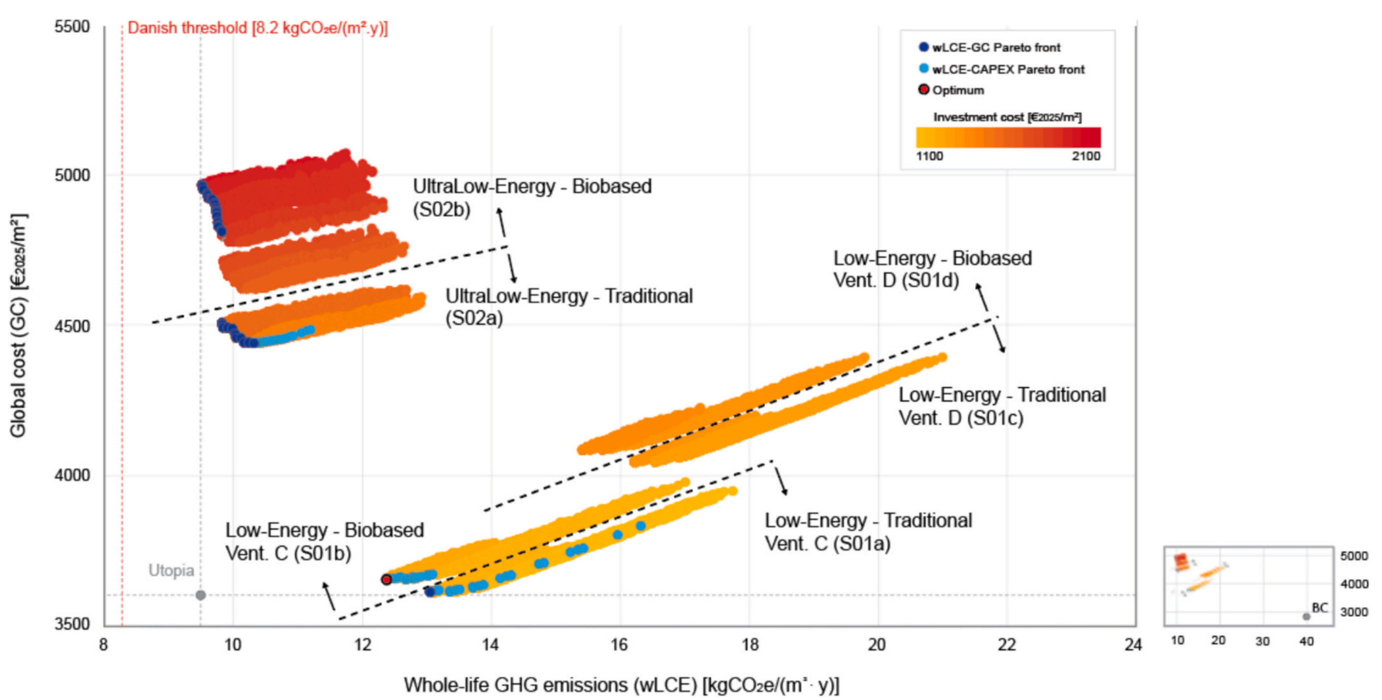

Fig. 3. Archetype A – Multi-objective optimization (MOO) results illustrating the trade-off between whole-life greenhouse gas emissions (wLCE) and global cost (GC). The color gradient indicates the investment cost (CAPEX) associated with each alternative. Dark blue points represent solutions included in the wLCE–GC Pareto front, while light blue points correspond to the wLCE–CAPEX Pareto front. (For interpretation of the references to colour in this figure legend, the reader is referred to the web version of this article.)

(35.7%), and 51 from S.02b (53.7%). All S.01 alternatives integrate heat pumps with a COP of 3.75 (10.6% of total Pareto solutions; 100% of S.01), while S.02 use COPs of 5 (5% of total; 6% of S.02), 5.25 (11% of total; 12% of S.02), and 5.50 (74% of total; 82% of S.02). PV panels with an efficiency of 0.16 are always included in S.01 (10.6% of total); those with 0.20 efficiency are always adopted in S.02 (89.4% of total). Glazing and doors have U-values of 0.8 in S.01, and 1.3 W/m^{2}K in S.02, with glazing g-values of 0.30 and 0.60, respectively. These features maximize solar gains to reduce heating energy use.

Airtightness is 0.04 ach in S.01 and 0.12 ach in S.02. For external walls and roofs, results are more dispersed. The lowest U-value (0.80 W/m^{2}K) appears consistently in S.01. In S.02, 0.15 W/m^{2}K is most common. Ground floor insulation peaks at 0.23 W/m^{2}K in S.02 solutions (39% of total; 44 of S.02). In S.01, values are more evenly spread, each representing 1/2% of total. These outcomes emphasize that system upgrades are generally more cost-effective than major envelope retrofits.

In contrast, the wLCE-CAPEX Pareto frontier (including 107 alternatives) favors S.01a (51) and S.01b (33) over the more advanced S.02a (23). The best-performing solutions are prioritized, but some exceptions occur. Ground floor insulation often remains at higher U-values: 84% of S.01 solutions falls between 0.36—–0.40 W/(m$^{2\cdot}$ K), representing 66% of the total. All S.02 solutions cluster at 0.23 W/(m$^{2\cdot}$ K), i.e., 20% of the total. Further improvement in this parameter yields minimal emissions cuts, yet demands much higher investments. Similarly, roof insulation peaks at 0.8 W/(m$^{2\cdot}$ K) (30% of the total, 38% of S.01). Another 49% of solutions (62% of S.01) are distributed between 0.88–1.00 W/(m$^{2\cdot}$ K). Finally, 96% of S.01 cases range from 0.3 to 0.4 W/(m$^{2\cdot}$ K).

Across both frontiers, Pareto post-processing (Section 2.4.3) reduced the set of 202 Pareto-optimal solutions to 12 representative options (Table 3). The best compromise, satisfying all combinations of renovation objectives (Section 2.4.3) and being the closest to the utopia, belongs to the S.01b scenario. This solution features a heat pump with a COP of 3.75, PV panel efficiency of 16%, glazing U-value of 1.3 W/(m$^{2\cdot}$ K) and g-value of 0.60, door U-value of 1.4 W/(m$^{2\cdot}$ K), ground floor U-value of 0.40 W/(m$^{2\cdot}$ K), roof and wall U-values of 0.80 W/(m$^{2\cdot}$ K), and airtightness of 0.12 ach. If cost is a major constraint (GIE and IGE scenarios), S.01a alternatives allow further reductions in both CAPEX and GC compared to S.01b, with two alternatives satisfying both GIE and IGE exigencies. Instead, S.02 does not appear competitive unless emissions are given priority in the scale of preferences.

Similar considerations apply to Archetype B (Fig. 4). In this case, however, CAPEX is 50% higher than in Archetype A, ranging from 1650 to 3200 €$_{2025}$/m^2. This is due to its smaller occupied area and less compact geometry, which significantly increases envelope-related renovation costs (Appendix A – Table A2). The lowest wLCE value amounts to 17.2 kgCO$_2$e/(m$^{2\cdot}$ y), about twice that of Archetype A, and would require an even more substantial reduction effort to meet the Danish threshold (−110%). Out of 74 Pareto solutions, the set was reduced to 11. The best compromise again belongs to strategy S.01b, with the same configuration: COP 3.75, PV efficiency 16%, glazing U-value 1.3 W/(m$^{2\cdot}$ K), g-value 0.60, door U-value 1.4 W/(m$^{2\cdot}$ K), ground floor U-value 0.40 W/(m$^{2\cdot}$ K), roof and wall U-values 0.80 W/(m$^{2\cdot}$ K), and airtightness 0.12 ach.

3.2. Payback period

From an environmental perspective (Fig. 6), the additional embodied emissions associated with retrofit interventions and future replacements (both combined in year 0) are offset after 14 to 30 years. The time frame depends on the solution and building archetype. In Archetype A, the payback period is shorter. The most advantageous solution is S.01b, followed by S.02b, S.02a, S.01a, S.01d, and S.01c. In Archetype B, the payback is longer, although S.01b remains the best-performing option. It is followed by S.01a, S.02b, S.02a, S.01d, and S.01c.

Over the reference study period, S.02b and S.02a demonstrate the best environmental performance in both archetypes. Their substantially lower operational emissions compensate for the higher embodied emissions, resulting in lower total life-cycle emissions. In contrast, S.01c and S.01d perform worse environmentally because of their high operational emissions.

From an economic standpoint, all retrofit solutions exhibit payback periods exceeding the 50-year study horizon (Fig. 7). The investment costs, combined with maintenance and replacement expenses, are not recovered through operational savings within this time frame. The relatively low cost of gas compared to electricity and the low carbon tax also limit reductions in operational costs. This makes the retrofit options economically unattractive for homeowners. However, analyzing the investment cost breakdown (Appendix A – Table A2) shows that

Table 3
Pareto Post-processing.

Renovation strategy	wLCE [kgCO$_2$e/(m$^{2\cdot}$ y)]	GC [€$_{2025}$/m^2]	CAPEX [€$_{2025}$/m^2]	GEI	GIE	EGI	EIG	IGE	IEG
Archetype A									
S.02b	9.46	4965	2130			✓	✓		
S.02a	9.77	4507	1703			✓	✓		
S.02a	9.79	4492	1687			✓	✓		
S.01b	**12.33**	**3780**	**1170**	✓	✓	✓	✓	✓	✓
S.01b	12.63	3780	1135	✓					
S.01a	13.00	3640	1129	✓	✓			✓	✓
S.01a	13.31	3635	1109	✓	✓			✓	
S.01a	13.67	3643	1105	✓	✓				
S.01a	13.83	3648	1103	✓	✓				
S.01a	14.26	3672	1101	✓	✓				
S.01a	15.38	3741	1095	✓	✓				
S.01a	16.27	3800	1093		✓				
Archetype B									
S.02b	17.23	7333	3170			✓	✓		
S.01b	**18.03**	**5360**	**1750**	✓	✓	✓	✓	✓	✓
S.01b	18.12	5356	1745	✓					
S.01a	18.70	5300	1720	✓	✓			✓	✓
S.01a	19.16	5292	1710	✓	✓			✓	✓
S.01a	19.31	5294	1706					✓	
S.01a	19.67	5299	1695	✓	✓			✓	
S.01a	19.84	5303	1692	✓	✓			✓	
S.01a	20.46	5337	1691	✓	✓				
S.01a	22.07	5434	1685	✓	✓				
S.01a	22.78	5479	1682	✓	✓				

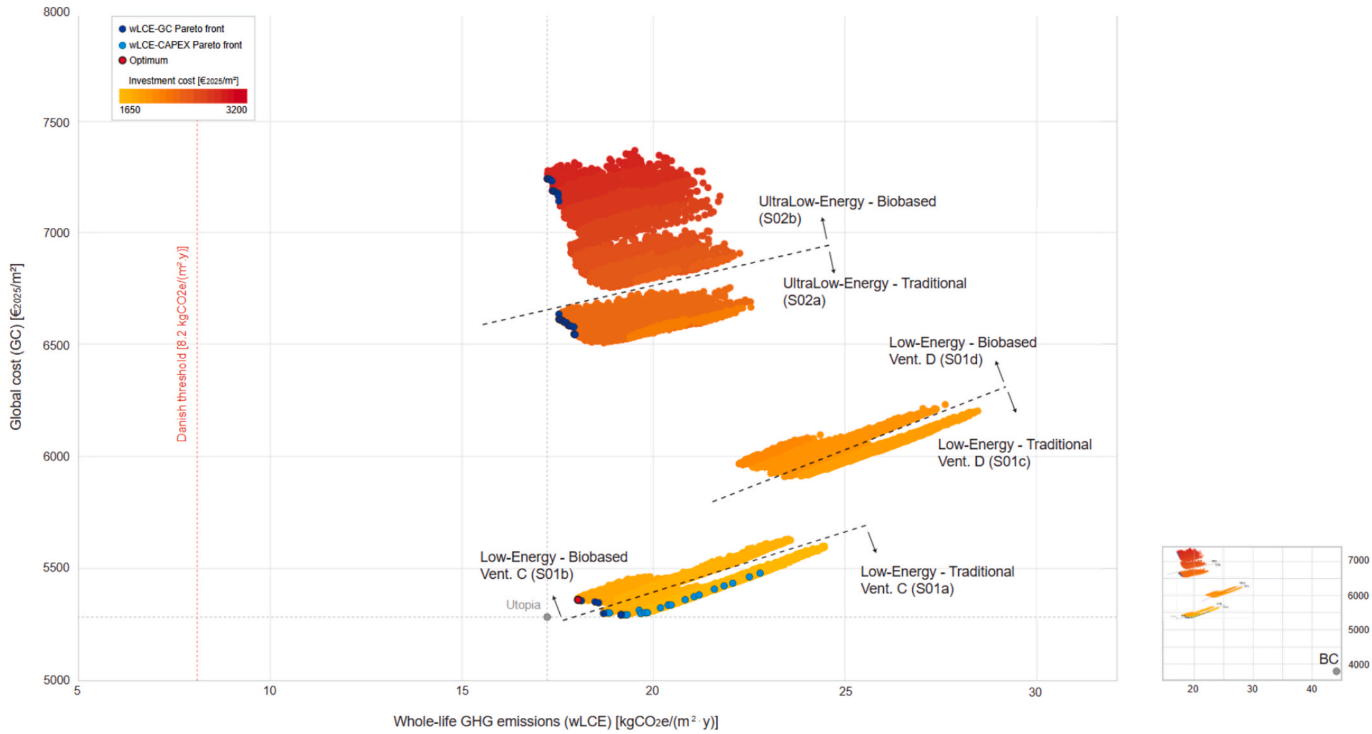

Fig. 4. Archetype B – Multi-objective optimization (MOO) results illustrating the trade-off between whole-life greenhouse gas emissions (wLCE) and global cost (GC). The color gradient indicates the investment cost (CAPEX) associated with each alternative. Dark blue points represent solutions included in the wLCE–GC Pareto front, while light blue points correspond to the wLCE–CAPEX Pareto front. (For interpretation of the references to colour in this figure legend, the reader is referred to the web version of this article.)

focusing solely on systems and storage retrofits could reduce the total investment by approximately 80%. This would significantly improve the payback period and make these targeted interventions more financially viable.

If the gas price is higher than electricity (the opposite of current conditions) and the carbon tax is double the 2050 level (800 $€_{2025}$/ton) from the start, the payback period would be achieved for Archetype A, also for S.02 (Appendix A – Fig. A.1). Furthermore, if they require a high level of performance, targeted subsidies would reduce the CAPEX gap with intermediate solutions (S.01) and make S.02 competitive. For this specific case, a subsidy of approximately 25% of S.02 retrofits would cover the CAPEX gap between S.01 and S.02, making S.02a even more attractive than S.01a in terms of payback period. Even in the long term, S.02a would become more competitive, although replacement costs place this alternative behind S.01a and S.01b.

On the other hand, acting only on subsidies does not allow the initial investment to be recovered within 50 years (Appendix A – Fig. A.2). Subsidies act only at the start of the lifecycle and do not ensure retrofit competitiveness over time, unlike carbon taxation and energy price mechanisms.

3.3. Effect of electricity mix projection on whole-life GHG emissions and global cost

Including future electricity mixes in the model, with a higher emission factor after 2030, raises both wLCE and GC. A more remarkable impact is registered for wLCE (Fig. 8). Mean wLCE increases by + 7.7/10.0% in the BC and by + 11.7/41.9% in the renovation scenarios compared to the static model with a constant electricity mix. In contrast, mean GC shows only minor variations, ranging from + 0.67% to + 0.95% in the BC and from + 0.41% to + 2.76% in the renovation scenarios. This limited variation in GC is explained by the low CO_2 price, which does not significantly penalize the doubling of the emission factor (Section 2.3.3).

Variations are generally greater in Archetype A than in Archetype B for both wLCE and GC, except in scenarios S.02a and S.02b. For wLCE, Archetype A shows greater variations despite lower net energy use intensity. Its compact geometry and larger occupied surface reduce the share of embodied emissions, so operational emissions become a larger portion of the total (Appendix A – Table A3). In scenarios S.02a and S.02b, however, Archetype B exhibits larger wLCE variations. This is driven by its lower PV production, which leads to higher net energy use and greater electricity imports than in Archetype A. Reduced PV exports halve the embodied PV emissions allocated to the grid (Section 2.2.2), thereby increasing the relative weight of embodied emissions. However, operational emissions still represent a larger share of the total in Archetype B. For similar reasons, mean GC shows a comparable trend: emissions-related costs account for a larger share in Archetype A than in B, except in S.02a and S.02b.

For both archetypes A and B, mean wLCE increases the most in S.01d and S.01c, then S.01b and S.01a, and finally S.02b and S.02a. This ranking mirrors net energy use: the greater the net energy use, the larger the impact of the evolving electricity mix. Biobased insulation alternatives consistently exhibit higher variability in wLCE than petrochemical ones. Although their net energy use is lower, biobased scenarios have a bigger share of operational emissions, due to lower embodied emissions. Conversely, biobased solutions show lower GC variability, as their higher upfront cost reduces the relative weight of energy-related emission costs. Thus, the greatest GC variations appear in S.01c and S.01d, followed by S.01a and S.01b, and lastly S.02a and S.02b.

Compared with renovation scenarios, the BC is least affected in both archetypes. wLCE increases by + 10.0% in Archetype A and + 7.7% in Archetype B. This is mainly because gas-powered heating limits electricity consumption, which dominates overall energy use. For GC, the BC ranks just after S.01b in Archetype A (+0.95%), since PV generation in S.02a and S.02b reduces net electricity consumption below that of the BC. In Archetype B, by contrast, the BC remains the least affected (+0.67%).

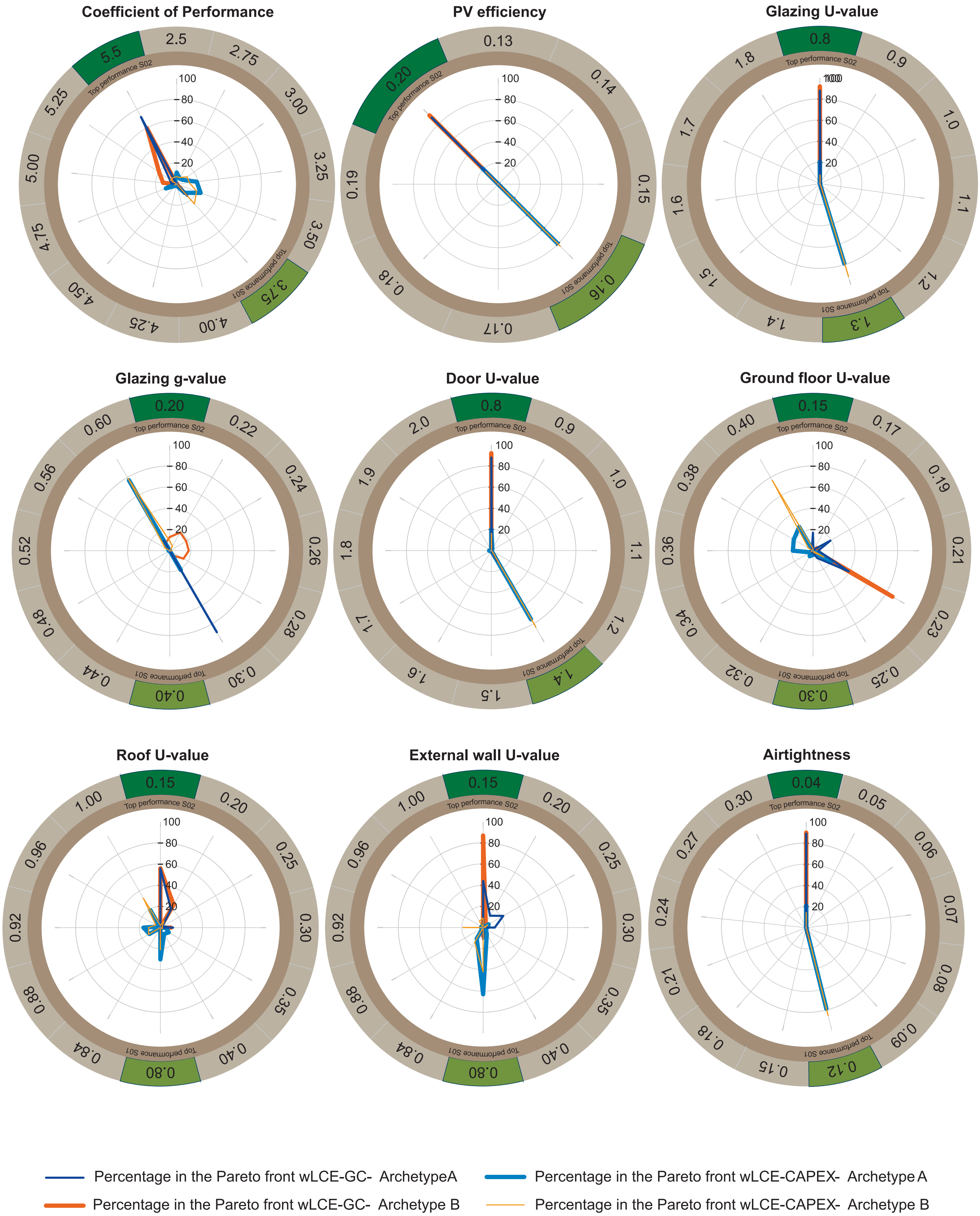

Fig. 5. Pareto analysis.

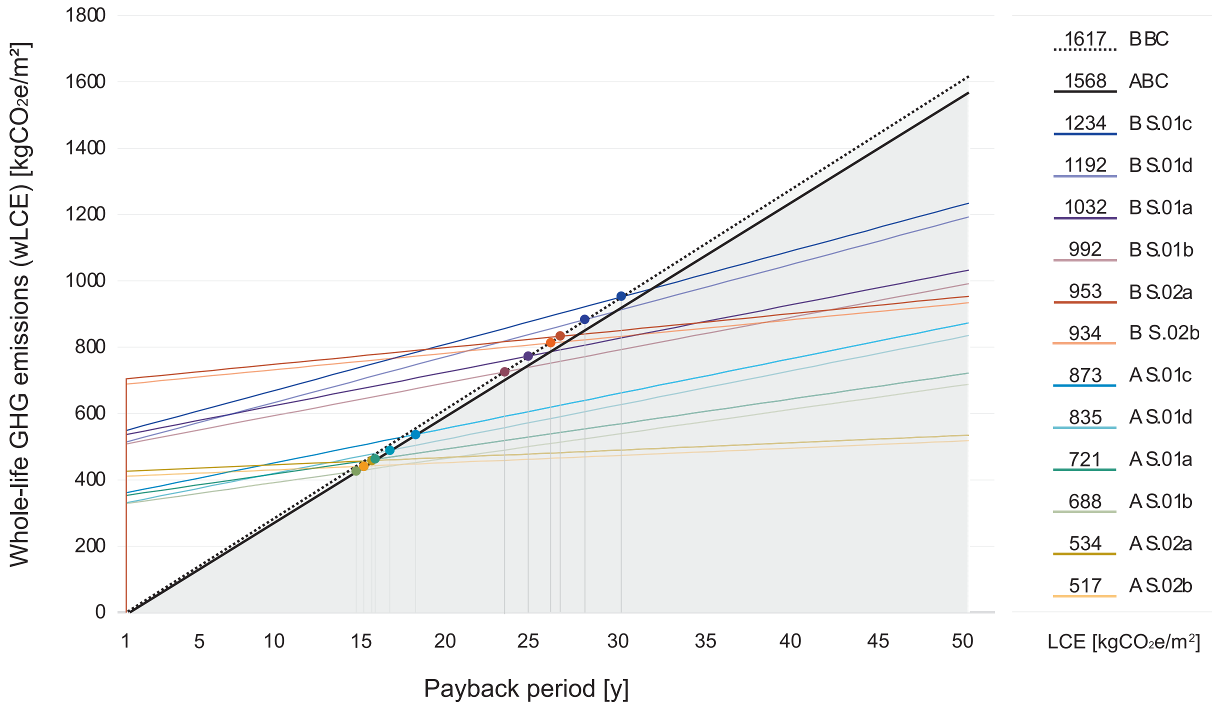

Fig. 6. Environmental payback period – Mean for each scenario.

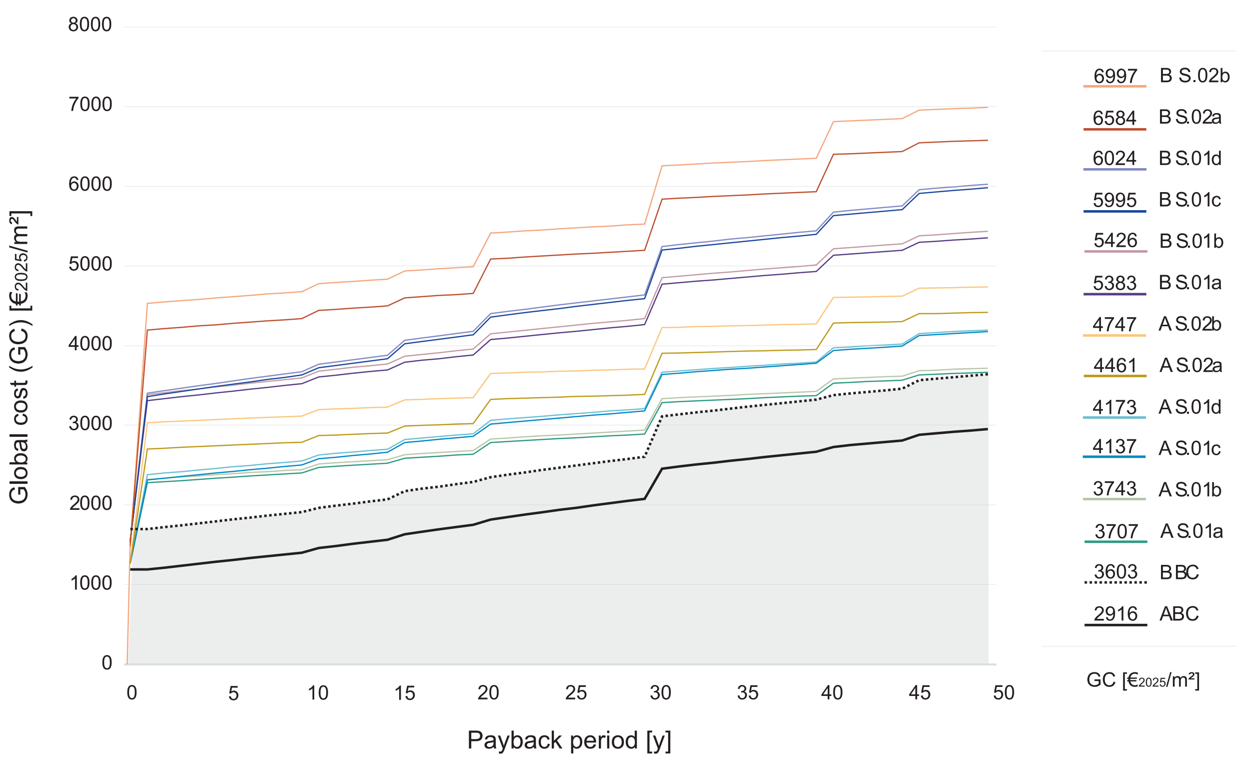

Fig. 7. Economic payback period – Mean for each scenario.

3.4. Effect of climate change on whole-life GHG emissions and global cost

The effects of climate change result in an overall reduction in both GC and wLCE, with a stronger impact on wLCE (Fig. 9). This reduction is mainly linked to decreased heating energy use. The increase in cooling energy use does not fully offset this decrease, resulting in lower operational emissions and costs. Mean LCE decreases by 21.6% to 39.1% in the BC, and by 5.6% to 21.0% in the renovation scenarios, compared with the static model that excludes climate change effects. Mean GC shows smaller reductions, ranging from –6.01% to –9.24% in the BC and –2.20% to –4.47% in the renovation scenarios.

The BC emerges as the most affected solution in both archetypes. This is due to high heating energy use, which increased cooling does not offset, unlike in renovation scenarios. Archetype B is more affected by

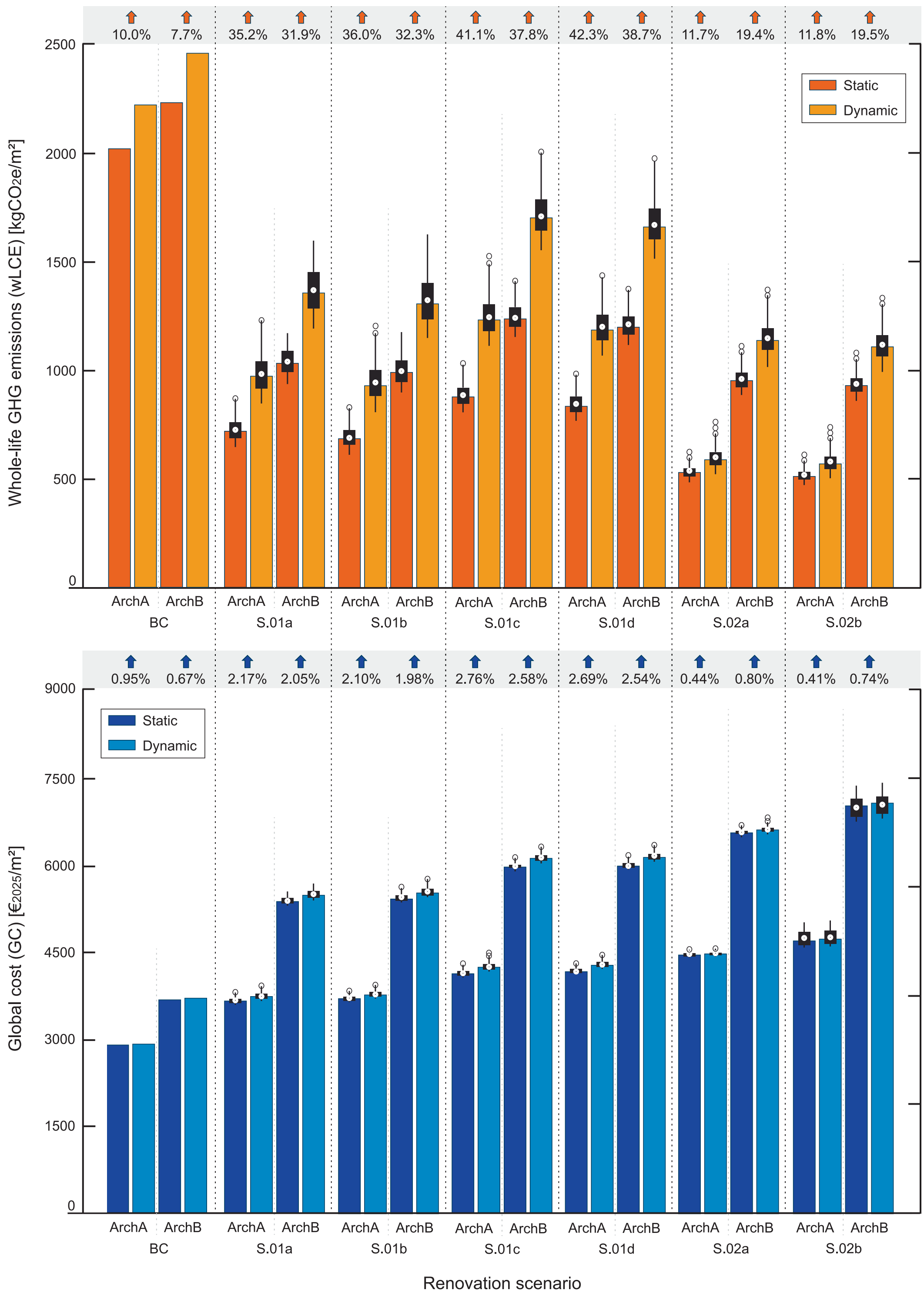

Fig. 8. Impact of electricity mix scenarios on global cost (GC) and whole-life GHG emissions (wLCE) in Archetypes A and B.

climate change than Archetype A. By 2070, heating energy use in Archetype B decreases by up to –35.8%, compared with –19.3% in Archetype A. This stronger reduction in B is likely due to its higher wall-to-floor ratio, larger roof surface with lower U-value, and less efficient heating system, which together make it more sensitive to variations in heating energy use. In renovation scenarios, this difference is attenuated since both archetypes share the same envelope and system performance, the introduction of cooling offsets part of the heating reduction, and PV production is lower in Archetype B than in Archetype A.

Within the renovation scenarios, the same trend highlighted in Section 3.3 is confirmed: wLCE and GC variations are generally larger for Archetype A than for Archetype B, due to the higher share of operational emissions in Archetype A (Appendix A – Table A3). The only exception is found in scenarios S.02. In these cases, climate change drives Archetype A into a net energy-negative balance, a shift not observed in Archetype B. This amplifies operational emission reductions in Archetype A, leading to larger decreases in both wLCE and GC.

The ranking of scenarios reflects these dynamics. For Archetype A, the largest wLCE reductions are observed in S.02b and S.02a. Next are S.01d and S.01c, followed by S.01b and S.01a. For Archetype B, the

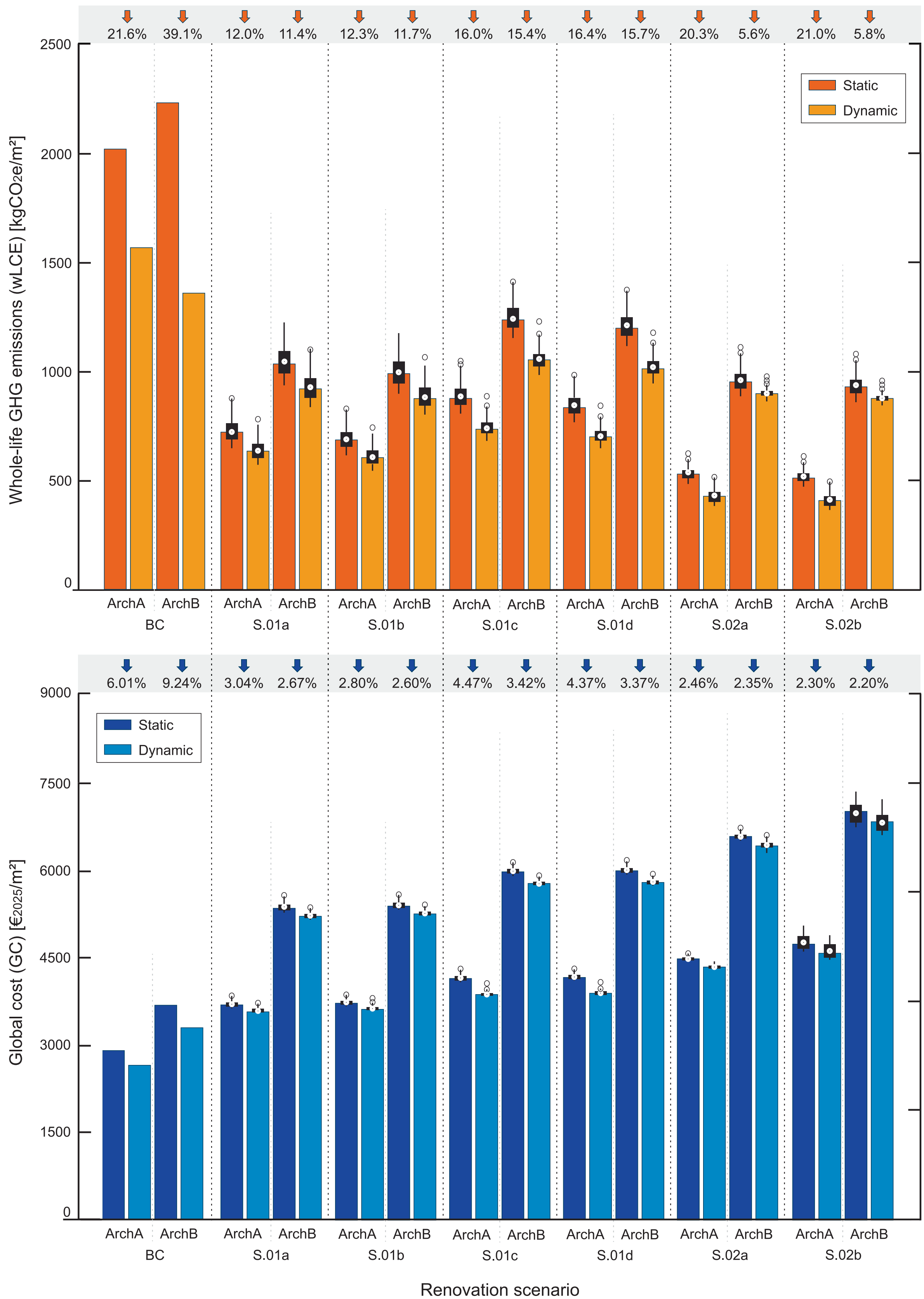

Fig. 9. Impact of climate change on GC and wLCE in Archetypes A and B.

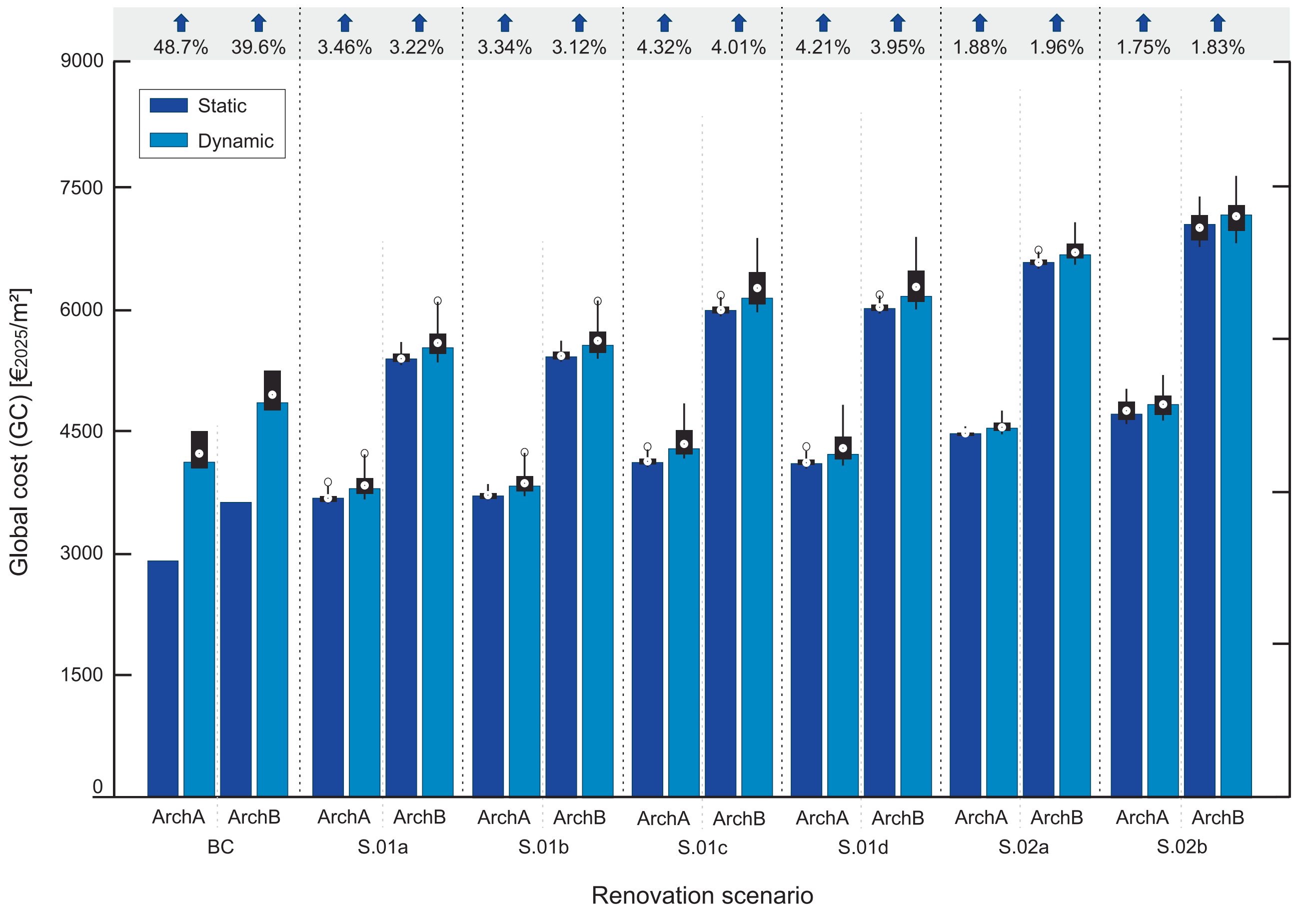

Fig. 10. Impact of energy price uncertainty on GC in Archetypes A and B.

strongest effects occur in S.01d and S.01c, then S.01b and S.01a. S.02b and S.02a show the smallest changes. GC rankings are more consistent across archetypes. The largest reductions occur in S.01c and S.01d, followed by S.01a, S.01b, S.02a, and S.02b. Both wLCE and GC rankings align with those obtained for the electricity mix uncertainty (Section 3.3). Biobased alternatives systematically show greater variability in wLCE but lower variability in GC than petrochemical solutions.

3.5. *Effect of energy price on global cost*

The integration of future electricity price scenarios (Section 2.4.2) results in a systematic increase in GC (Fig. 10), driven by rising gas and electricity prices and by the removal of benefits from surplus electricity sold to the grid.

BC emerges as the most impacted solution in both archetypes, with increases of + 48.7% in A and + 39.6% in B. This outcome reflects the BC's high energy use, which makes it especially vulnerable to fluctuations in energy prices. Renovation scenarios are less affected, although the magnitude of variations depends on the archetype and scenario considered.

Overall, cost variations are greater in Archetype A than in Archetype B, except in scenarios S.02a and S.02b, in accordance with the trend in emissions-related costs evidenced in Section 3.3. The ranking confirms this logic. For both archetypes, the largest GC increases occur in S.01c (+4.32/+4.01%) and S.01d (+4.21/+3.95%), followed by S.01a (+3.46/+3.22%) and S.01b (+3.34/+3.12%), and finally S.02a (+1.88/+1.96%) and S.02b (+1.75/+1.83%).

In addition to increasing average GC, considering multiple energy price scenarios increases the uncertainty of the result. This is evident in the wider gap between minimum and maximum GC, highlighting the sensitivity of long-term cost estimates to future energy market dynamics.

3.6. *Effect of occupants' behavior on whole-life GHG emissions and global cost*

Uncertainty in heating and cooling setpoints affects wLCE and GC differently across scenarios and archetypes (Fig. 11). In Archetype A, most alternatives show a reduction in both indicators, with the exception of S.02a and S.02b. In Archetype B, reductions are more limited in S.01a and S.01b, while an opposite trend (increase in wLCE and GC) is observed in the other alternatives.

These results arise from the interplay of multiple factors. First, heating setpoints are on average higher in Archetype A than in Archetype B (Appendix A – Table A1). In Archetype B, indoor temperatures never exceed 22 °C, so combinations with a 23 °C heating setpoint in the UA increase heating demand compared with the static baseline. Second, in cases showing an increase in average wLCE, this effect is mainly driven by the increase in mechanical ventilation energy use: lower indoor temperatures reduce the effectiveness of heat recovery in winter, which in turn raises heating coil demand and offsets reductions in heating and cooling loads.

Across both archetypes, System D solutions are the least affected, followed by S.01b and S.01a. In contrast, BC is the most affected, consistent with its lower energy performance. As observed in previous analyses, bio-based alternatives show slightly higher sensitivity in terms of wLCE due to their larger share of operational emissions; however, they exhibit lower variability in GC owing to their higher upfront and non-energy-related costs.

The impact of setpoint uncertainty is particularly visible in the

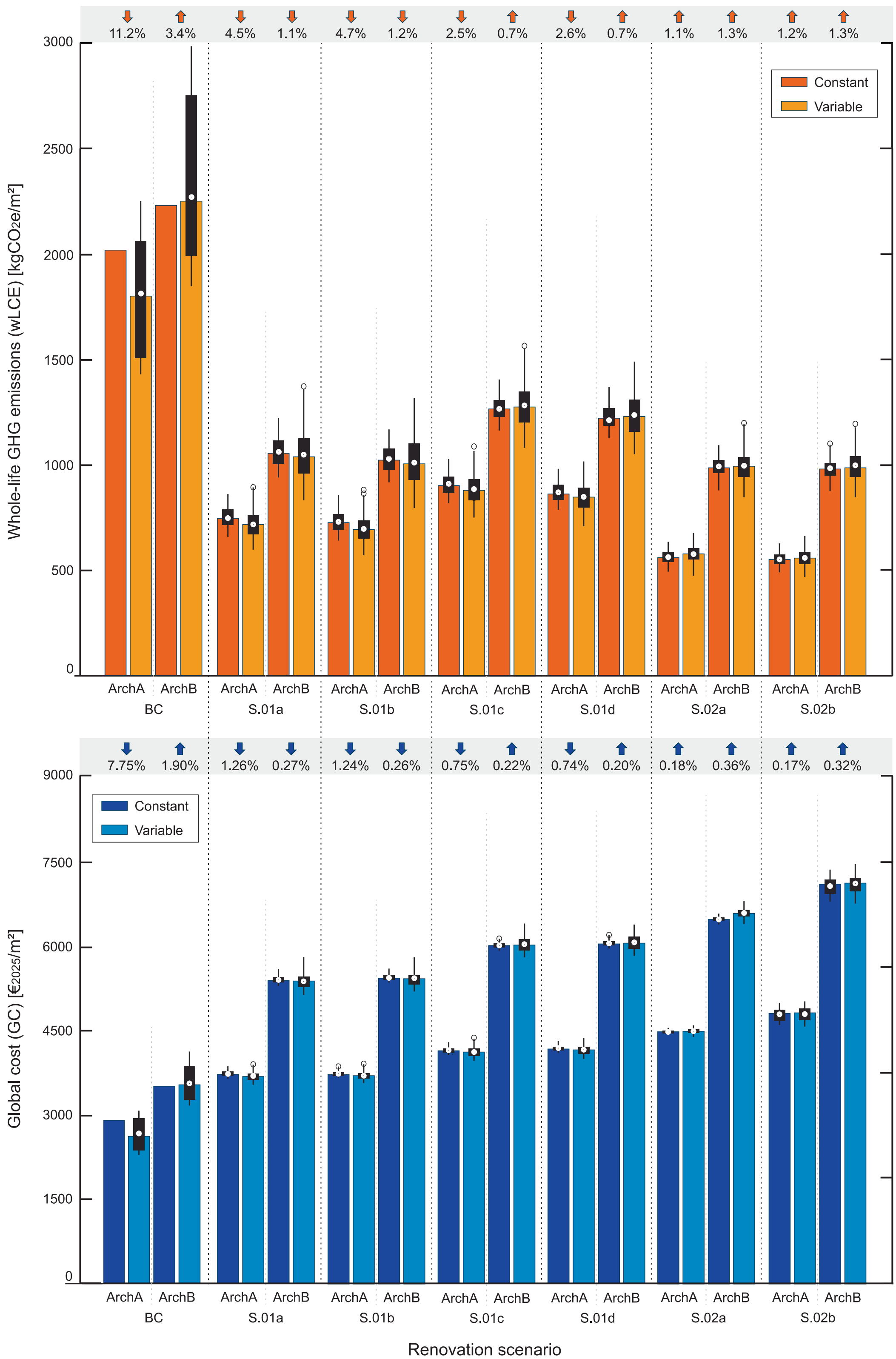

Fig. 11. Impact of temperature setpoint uncertainty on GC and wLCE in Archetypes A and B.

coefficient of variation (CV), especially for wLCE. For BC, CV reaches 15.76% in Archetype A and 15.73% in Archetype B. The lowest values are observed in S.02a (6.55%) and S.02b (6.80%) in Archetypes A and B, respectively (Fig. 15). These results highlight substantial variability from heating and cooling setpoint assumptions, making less efficient alternatives the most affected.

A shift from an elderly couple to a family of four changes how space is used and affects conditioning needs. The second bedroom is now occupied, so the conditioned floor area expands. Heating and cooling setpoints are adjusted (21 °C for heating, 25.5 °C for cooling). There are also more appliances, and they are used more each day.

These changes lead to significant differences in energy demand.

Lighting use grows by 32% in S.02a,b of Archetype A and 56% in other scenarios. Equipment energy use jumps by 214% in Archetype A and 105% in Archetype B. Mechanical ventilation use also rises, especially in Type D systems. It goes up by 40% in S.01a, 45% in S.01b, 88% in S.01c and S.01d, and 13% in S.02a and S.02b for Archetype A. For Archetype B, it increases by 67% in S.01c and S.01d, and 73% in S.02a and S.02b. Only S.01a and S.01b of Archetype B show a small drop (–5%). Cooling demand rises sharply in almost all cases, between 387 and 571% in Archetype A and 71–395% in Archetype B. Conversely, heating demand usually falls: –8% in S.01a and S.01b, –30% in S.02a and S.02b in Archetype A, and –22% in S.01a and –19% in S.01b in Archetype B. In Archetype B, lower heating offsets higher use from other sources, so net energy use, operational emissions, and GC fall (Fig. 12). In other scenarios, total building energy demand increases more than heating drops, leading to higher emissions and less power exported to the grid. This reduces the benefits of sharing PV embodied emissions with the grid, raising wLCE (Section 2.2.2).

The BC scenario is an exception. Here, energy use falls, especially in Archetype B, while GC rises. This apparently counterintuitive result stems from lower heating and DHW demand supplied by the gas boiler, that are compensated by higher lighting and equipment electricity use. In fact, electricity costs much more than gas (Section 2.2.3), offsetting the savings.

3.7. Effect of materials service life on whole-life GHG emissions and global cost

Substituting fixed service-life values with realistic ranges for components (Section 2.3.3, Table 2) results in a consistently increases both wLCE and GC across all scenarios (Fig. 13).

For wLCE, the average increase ranges from + 0.6% in S.01c and S.01d (both Archetypes) to + 1.4% in S.02a,b in Archetype A and + 1.7% in S.02a in Archetype B. This progression illustrates the joint impact of material intensity (highest in S.02 scenarios and lowest in S.01c,d) and the share of embodied emissions. The latter remains higher in scenarios adopting traditional materials versus biobased options, and higher in Archetype B than in Archetype A.

For GC, the trend is more complex. Biobased scenarios are generally more affected than petrochemical ones, except in S.01a and S.01b. In S.01a, average costs increase by + 5.37% in Archetype A and + 6.63% in Archetype B. In comparison, S.01b shows increases of + 4.90% and + 5.90%, respectively. This behavior is explained by the greater share of replacement costs in GC for traditional-materials scenarios. This variability in the share of replacement cost can also explain the variability in which Archetype A or B dominates within the same renovation scenario.

The BC scenario is less influenced, as it lacks insulation, mechanical ventilation, on-site renewable energy generation, and associated storage systems.

The CVs, ranging from 8.7 to 13.1% for wLCE and from 2.3 to 23.9% for GC (Fig. 15), highlight the additional uncertainty introduced by service life variability, particularly for the most material-intensive alternatives (S.02b).

3.8. Effect of materials quantity on whole-life GHG emissions and global cost

Uncertainty in material quantities does not affect the average values of wLCE and GC (Fig. 14). Quantities, calculated per m^2, were varied uniformly by ± 10%, so emissions and costs rose proportionally. However, uncertainty amplifies variability in results, with a slightly greater effect on wLCE than on GC. The CV increases with the material intensity of renovation scenarios and with the relative importance of embodied emissions and renovation costs (investment, renovation, and disposal) on the total.

In Archetype A, the CV for wLCE rises from 6.11% in S.01d to 10.19% in S.02b, while for GC increases from 5.42% in S.01a to 8.11% in S.02b (Fig. 15). In Archetype B, CV values grow from 6.26% in S.01d to 9.00% in S.02b for wLCE and from 5.66% in S.01c to 7.82% in S.02b for GC.

Fig. 15 summarizes the UA results. For both Archetypes, the parameters with the greatest impact on the average wLCE are the electricity mix projections, occupancy type, and climate change. In terms of CV, the most influential parameters are the temperature setpoint, material quantities, and materials' service life.

Regarding cost, the energy price and materials' service life exert the strongest influence on the average GC. From the CV perspective, materials' service life, quantities, and temperature setpoint are key parameters. No scenario appears particularly vulnerable to uncertainty. The greatest variations occur in BC and S.02b, which are the most energy- and material-intensive scenarios. Using the post-processing approach from Section 3.1, it solution S.01a is the most preferred for all UA samples.

4. Discussion

4.1. Results and recommendations

The results of this study indicate that achieving net-zero GHG emissions in the building stock through renovation remains highly challenging under current technical, economic, and policy conditions. A clear trade-off emerges between emissions reductions and economic performance: deeper retrofits generally yield greater GHG emissions savings but are associated with higher capital expenditures and GC. In terms of emissions, the best energy-performing and bio-based alternative (S.02b) should be preferred. Nevertheless, none of the evaluated retrofit strategies allows buildings to meet the Danish GHG emissions threshold, which itself is formulated for new construction rather than renovation. A substantial emissions gap therefore remains, with required wLCE reductions ranging from 13% to 110% for the best-performing retrofit scenarios of Archetypes A and B, respectively. This result shows the need for systemic change beyond the building sector, with investment in the energy supply and in the supply chain decarbonization, to reduce both operational emissions from buildings and embodied emissions from materials.

From a cost perspective, no renovation or system-focused interventions appear to be the most feasible solutions in the current context. This is due to the high upfront cost of complete renovations, which cannot be recovered within a reasonable time frame (Fig. 7). This is particularly evident in less compact building geometries (Archetype B), where envelope renovation accounts for up to 50% of the total retrofit investment.

Analysis of the Pareto frontier confirms this trend: most non-dominated solutions adopt high-efficiency heat pumps and PV panels, while extensive envelope insulation measures are generally not required to achieve near-optimal performance. These findings are consistent with Bertini et al. [7], who identified the heat pump COP and, for advanced renovation levels, PV system performance, as the most influential parameters affecting wLCE, followed by envelope improvements.

In contrast, in a hypothetical situation where the gas/electricity price ratio would be reversed from the current situation, and where CO_2 emissions taxation would double what is currently planned for 2050, the retrofit investment would be largely recovered for Archetype A, also for the most unfavorable S.02 scenario. However, S.01 alternatives remain the most favorable. To move towards greater decarbonization, it would be necessary to target subsidies for high-performance insulation and systems to reduce the gap with S.01 alternatives and make S.02 competitive, also from an economic point of view.

Among the investigated options, solution S.01b represents the best compromise between GC, wLCE, and investment cost for both archetypes. Solution S.01a is a better option if greater cost constraints are imposed, while alternatives S.02 are not competitive in the current context.

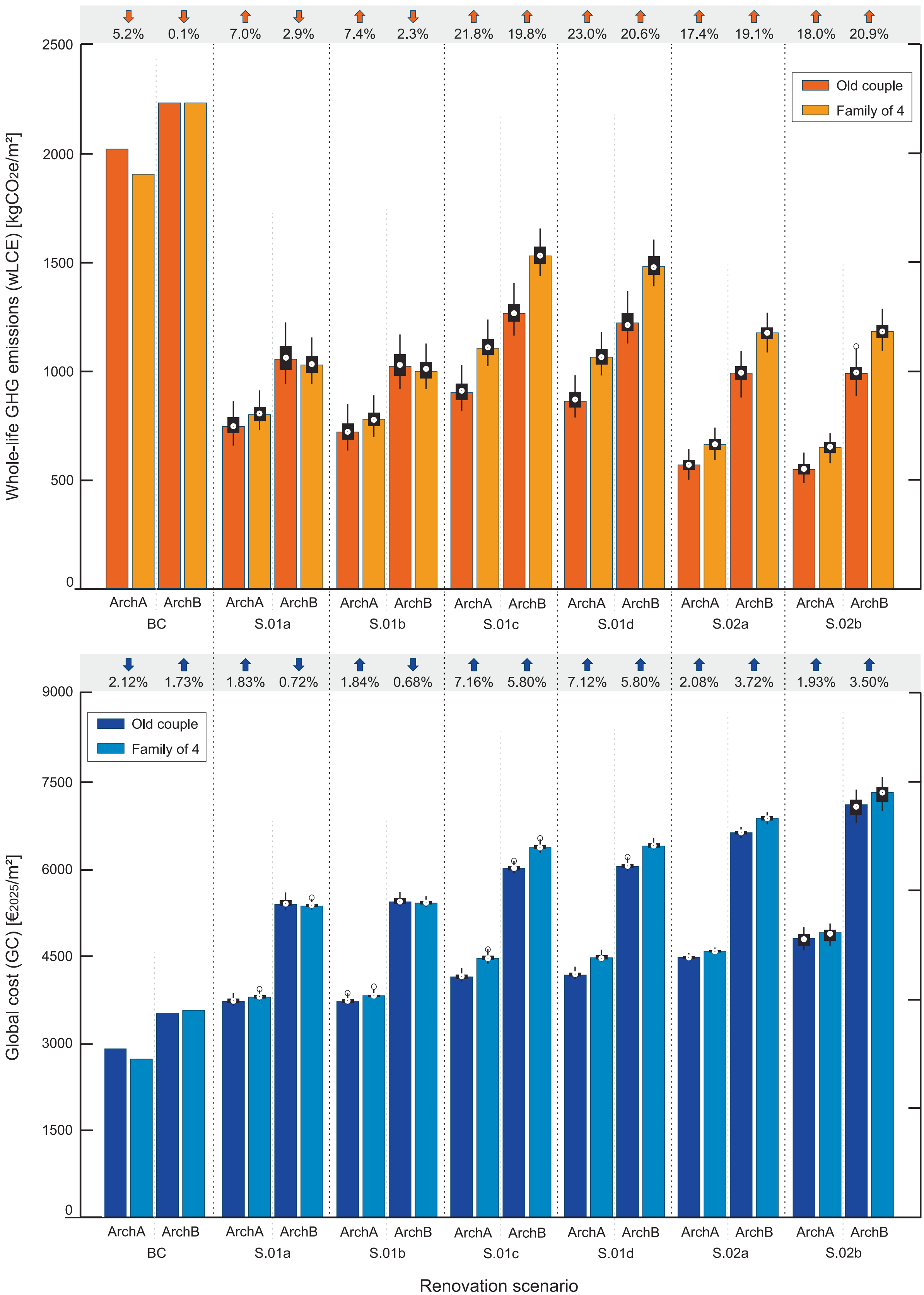

Fig. 12. Impact of occupancy type on GC and wLCE in Archetypes A and B.

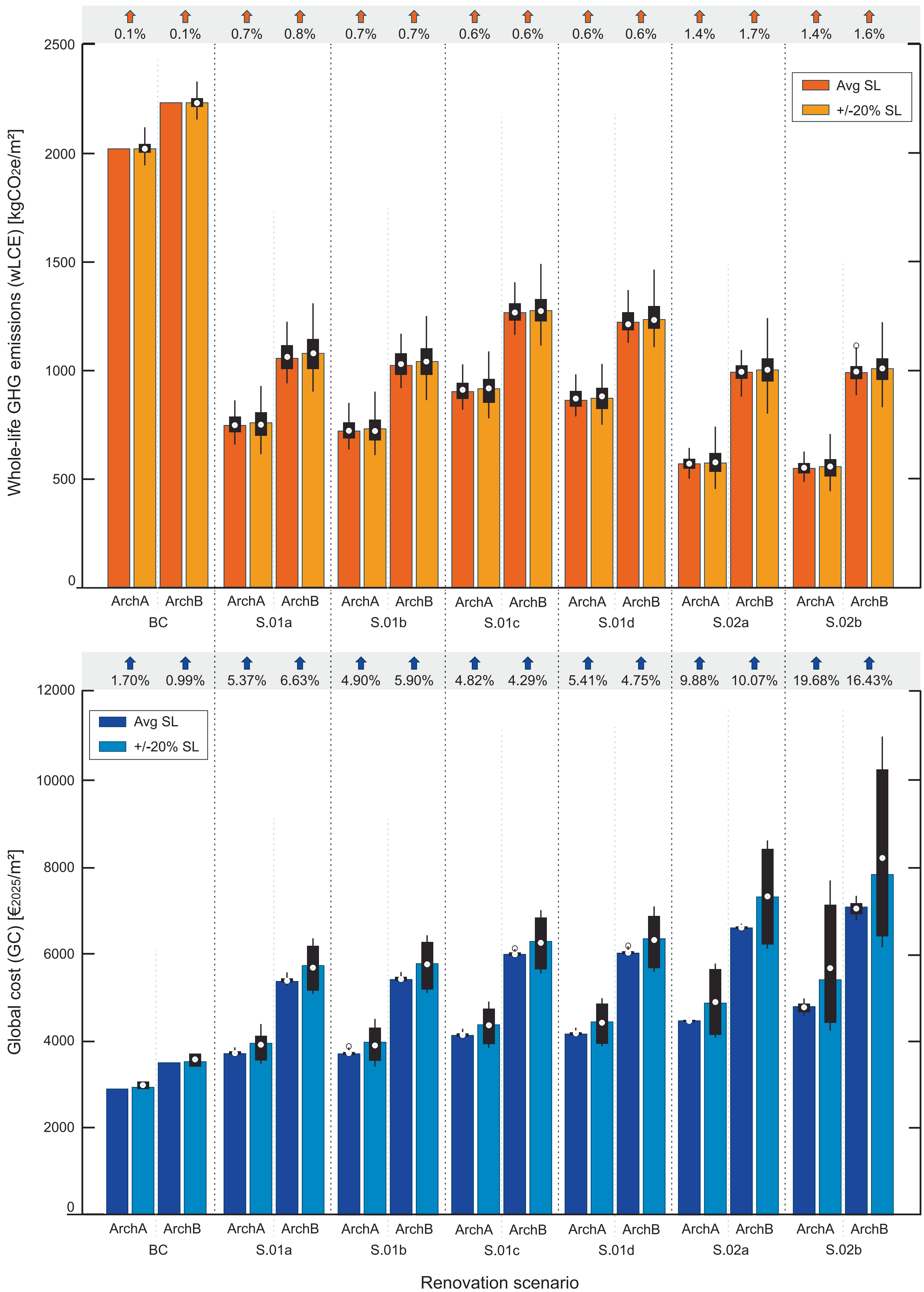

Fig. 13. Impact of service life uncertainty on GC and wLCE in Archetypes A and B.

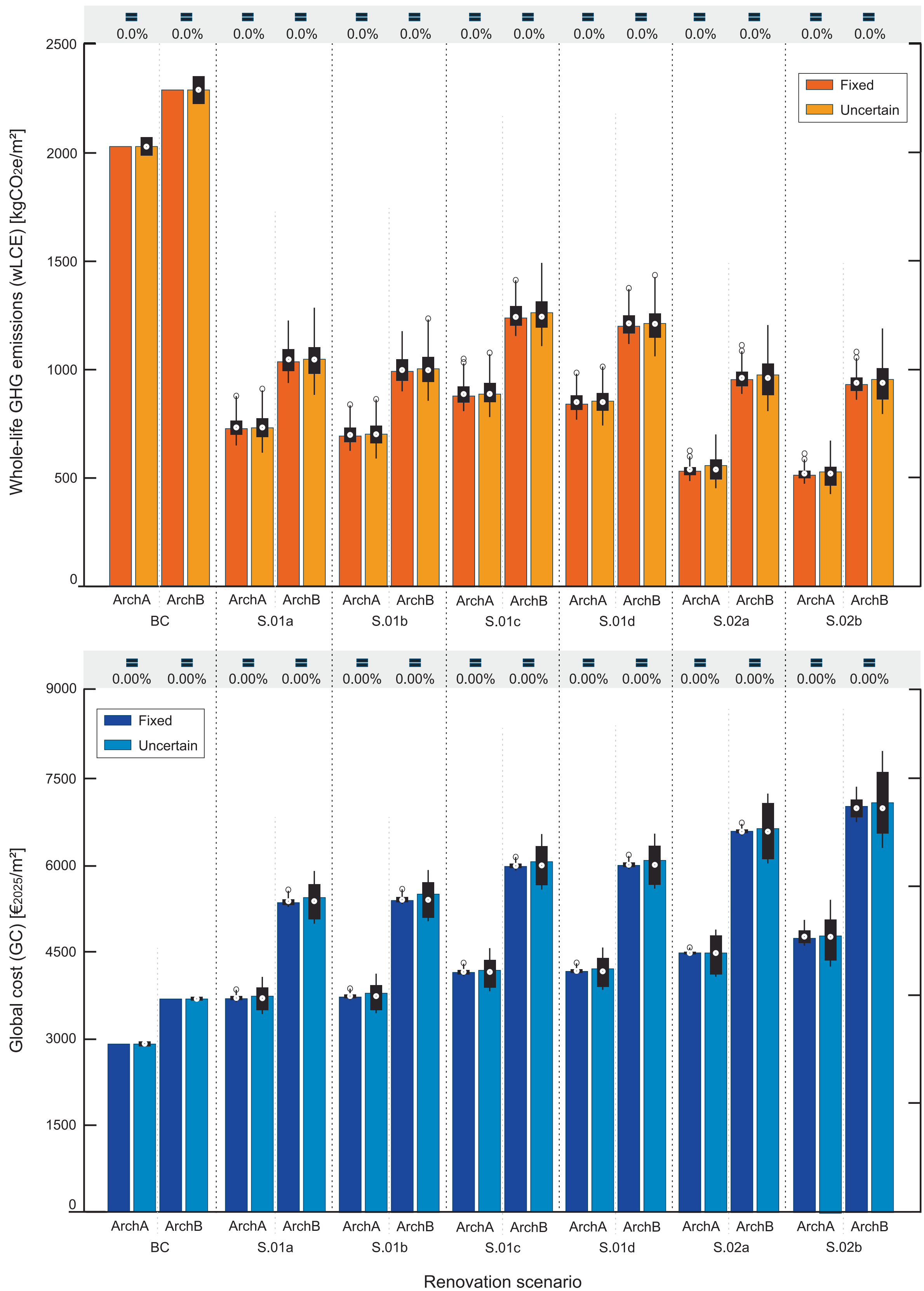

Fig. 14. Impact of materials quantity uncertainty on GC and wLCE in Archetypes A and B.

Scenario	Electricity mix	Climate change	Energy price	Temp. setpoint	Occupancy	Materials service life	Materials quantity
Archetype A – Average wLCE							
BC	10	-21.6	/	-11.2	-5.2	0.1	0
S.01a	35.2	-12	/	-4.5	7	0.7	0
S.01b	36	-12.3	/	-4.7	7.4	0.7	0
S.01c	41.1	-16	/	-2.5	21.8	0.6	0
S.01d	42.3	-16.4	/	-2.6	23	0.6	0
S.02a	11.7	-20.3	/	1.1	17.4	1.4	0
S.02b	11.8	-21	/	1.2	18	1.4	0
Archetype B – Average wLCE							
BC	7.7	-39.1	/	3.4	-0.1	0.1	0
S.01a	31.9	-11.4	/	-1.1	-2.9	0.8	0
S.01b	32.3	-11.7	/	-1.2	-2.3	0.7	0
S.01c	37.8	-15.4	/	0.7	19.8	0.6	0
S.01d	38.7	-15.7	/	0.7	20.6	0.6	0
S.02a	11.7	-5.6	/	1.3	19.1	1.7	0
S.02b	11.8	-5.8	/	1.3	20.9	1.6	0
Archetype A - Average GC							
BC	0.95	-6.01	48.7	-7.75	-2.12	1.7	0
S.01a	2.17	-3.04	3.46	-1.26	1.83	5.37	0
S.01b	2.1	-2.8	3.34	-1.24	1.84	4.9	0
S.01c	2.76	-4.47	4.32	-0.75	7.16	4.82	0
S.01d	2.69	-4.37	4.21	-0.74	7.12	5.41	0
S.02a	0.44	-2.46	1.88	-0.18	2.08	9.88	0
S.02b	0.41	-2.3	1.75	-0.17	1.93	19.68	0
Archetype B - Average GC							
BC	0.67	-9.24	39.6	1.9	1.73	0.99	0
S.01a	2.05	-2.67	3.22	-0.27	-0.72	6.63	0
S.01b	1.98	-2.6	3.12	-0.26	-0.68	5.9	0
S.01c	2.58	-3.42	4.01	-0.22	5.8	4.29	0
S.01d	2.54	-3.37	3.95	-0.2	5.8	4.75	0
S.02a	0.8	-2.35	1.96	-0.36	3.72	10.07	0
S.02b	0.74	-2.2	1.83	-0.32	3.5	16.43	0

Scenario	Electricity mix	Climate change	Energy price	Temp. setpoint	Occupancy	Materials service life	Materials quantity
Archetype A - CV wLCE							
BC	0	0	/	15.8	0	8.7	2.1
S.01a	8.4	6.3	/	8.9	4.9	8.7	8.4
S.01b	8.2	6.3	/	8.7	4.9	9.8	8.2
S.01c	6.6	4.7	/	7.7	4.2	9.8	6.9
S.01d	6.5	4.7	/	7.5	4.2	9.8	6.1
S.02a	8.1	6.6	/	6.6	4.6	9.5	10.1
S.02b	8.3	6.8	/	7	4.5	9.5	10.2
Archetype B – CV wLCE							
BC	0	0	/	15.73	0	9	2.8
S.01a	7.9	6	/	10.97	4.6	9.9	8.1
S.01b	8	6	/	11.25	4.6	10	8.16
S.01c	5.5	3.8	/	7.88	3.3	9.9	6.34
S.01d	5.5	3.9	/	7.74	3.4	9.2	6.26
S.02a	6.3	2.3	/	7.19	3	13.1	8.99
S.02b	6.3	2.3	/	6.8	3.5	12.6	9
Archetype A - CV GC							
BC	0	0	4.9	10.44	0	2.3	2
S.01a	1.7	1.2	3.4	2.12	1.1	9	5.42
S.01b	1.5	1	3.2	1.94	1	9.9	5.94
S.01c	1.5	0.9	3.9	2.1	1.1	9.6	5.88
S.01d	1.3	0.8	3.8	1.89	1	10.4	6.38
S.02a	0.7	0.7	1.4	0.9	0.5	15.6	7.57
S.02b	2.5	2.6	2.7	2.37	2	23.9	8.11
Archetype B - GC							
BC	0	0	4.7	8.88	0	4	2.1
S.01a	1.4	0.9	3.1	2.68	0.8	9	5.7
S.01b	1.4	0.9	3	2.63	0.8	9.5	5.76
S.01c	1.1	0.7	3.6	2.14	0.8	9.6	5.66
S.01d	1	0.7	3.5	2.04	0.7	10.1	5.69
S.02a	0.7	0.9	1.6	1.16	0.7	15	7.33
S.02b	2.2	2.2	2.5	2.18	2	23	7.82

Fig. 15. Uncertainty analysis results: average variation (left) and CV (right) of wLCE and GC per parameter and renovation scenario.

Parameter uncertainty further complicates the decision-making process. Energy price variability has the strongest influence on GC (particularly in the most energy-intensive scenarios), while electricity mix projections, occupancy type, and climate change significantly affect the wLCE results (Fig. 15). Temperature setpoints, materials service life, and materials quantities strongly impact both indicators. Post-processing of the UA results indicates S.01a as the more robust retrofit alternative, unlike the MOO post-processing, which suggested S.01b as the best compromise. It is therefore essential to incorporate these parameters into the decision-making process to ensure robust retrofit solutions.

To avoid compromising the benefits of renovation during the use phase, results suggest that equally important is to educate, engage, and incentivize occupants on proper building operation and maintenance, through a process that not only offers training and explains the importance of resource efficiency measures, but also incentivizes occupants through the behavior change process, such as material prizes or symbolic rewards [56]. With the same purpose, to avoid excessively increasing or decreasing the heating and cooling setpoint, adaptive comfort strategies should be considered during the design process to ensure a comfortable indoor environment that minimizes overreaction to environmental discomfort via thermostat variations. This might include the possibility to operate windows to regulate the volume of fresh air or movable solar shadings that allow occupants to control solar gains.

These measures may be integrated with control systems to mitigate the uncertainty related to occupants' behavior, allowing for more robust systems design that is less exposed to user behavior uncertainty. Although this would require a higher initial investment, it would reduce the uncertainty of results and preserve the permanent benefits gained from the building renovation. Examples of such interventions might include: occupant-centered intelligent thermostats that learn occupant preferences, occupancy patterns, and adjusts thermostat set-points accordingly to increase occupant comfort and optimize HVAC performance [36]; automated operable windows that notifies occupants of prime conditions to open their windows to balance energy efficiency and indoor air quality [56]; or automated solar shadings that allow control of solar gains according to interior and exterior conditions, while preserving the occupants' satisfaction [8].

In conclusion, the findings suggest two key renovation pathways:

- When considering only cost, no renovation is advisable under current conditions, as renovation costs cannot be recovered within the building's lifetime.
- If renovation is undertaken, system upgrades should be prioritized (even though they may be less effective or difficult to justify in poorly insulated buildings [35], as they offer better payback opportunities. By contrast, envelope renovations pose significant economic challenges.

As also remarked by Ruellan et al. [53], without upfront investment combined with stronger incentives, retrofits remain unaffordable. Moreover, exponential increases in operational energy costs arising from carbon taxation, improvements in workforce training, or mortgage policy reform are necessary to maintain retrofits' competitiveness through the lifecycle. Without such a paradigm shift, it is doubtful that large-scale deep renovation will take off.

4.2. Strengths, limitations and future work

The major strength of this study lies in integrating whole-life cycle assessment, BPS, and LCC into a coherent framework for evaluating retrofit strategies and simultaneously examining the effects of parameter uncertainty on GC and wLCE. Another strength is the wide scope, including retrofit of the envelope, systems, and on-site renewables. The analysis covers the stages A0-A5, B4, B6, C3-C4, justifying the term whole-life cycle assessment. Finally, Pareto post-processing and dynamic modelling strengthen results robustness and enable more accurate evaluation of cost–emissions trade-offs.

Several limitations must be acknowledged. This framework was developed based on the sensitivity analysis conducted by Bertini et al. [7], which enabled the prior identification of the most influential parameters to include in the building retrofit analysis. This targeted parameter selection helped limit model complexity and maintain computational time within a reasonable range, at approximately 2–3 min per generation of 40–50 cases. Nevertheless, the framework may still be computationally demanding when applied to the full analysis, potentially limiting its practical applicability for practitioners.

Second, the analysis is specific to the Belgian context. Although the methodological framework can be applied to other countries, the results may not be directly transferable to other regions with different building characteristics, climatic conditions or policy frameworks. Particularly, while uncertainty in occupants' behavior was assessed based on ISO 18523–2, and materials service life was based on EN 15459–1, and thus findings might be broadly transferable, energy, labor and material prices, electricity mix and its decarbonization pathways, and future climate scenarios are context-specific, limiting the extension of results to other countries. For instance, in countries where the electricity mix is more decarbonized than Belgium (e.g., France), high initial embodied emissions would take longer to offset. Similarly, in cooling-dominated countries, greater attention should be paid to cooling demand in future climate change scenarios. In these regions, an investment in PV panels and storage systems may be more attractive than in Belgium. This would allow to compensate for the increased demand for cooling and ensure less dependence on a grid that is expected to be more vulnerable to electricity shortages.

Finally, effects of electricity mix variations on material production costs and improvements in renewable energy, which could reduce costs and boost market adoption, were not included. Also, the dynamic models did not account for material performance degradation over time. This may affect long-term results.

Future research should address the identified limitations by expanding the scope beyond Belgium. It should also include variations in the electricity mix, changes in renewable technology costs, and material degradation over time. At the technological level, digital twins and advanced algorithms could further improve modelling accuracy and operational optimization. From an economic perspective, detailed analyses of financing mechanisms are needed to assess their impact on retrofit uptake.

5. Conclusion

This study presented an integrated methodological framework combining dynamic LCA, BPS, and LCC within MOO and UA. This novel approach identified renovation strategies for residential buildings that provide the best compromise between cost and emissions. Through UA and the joint assessment of environmental and economic indicators, it also quantified how archetype characteristics, occupant behavior, and future climatic and energy conditions jointly influence both economic and environmental outcomes. This framework also allowed for explicit policy-oriented interpretation of the results.

The analysis revealed that retrofit solutions can substantially reduce wLCE. However, none of the investigated options achieves the Danish GHG threshold for new constructions. An emission gap of 13% and 110% remains for the best alternatives of Archetypes A and B, respectively. Building decarbonization thus seems to require action beyond the building perimeter, including further decarbonization in materials supply chains and electricity grids to meet set emission thresholds.

The trade-off between emissions reduction and cost is evident. CAPEX rises from 1100 to 2140 $€_{2025}/m^2$ in Archetype A, and from 1650 to 3200 $€_{2025}/m^2$ in Archetype B, when moving from retrofit scenario S.01a to S.02b. This clearly shows that higher environmental performance requires greater investments and longer payback times.

The most cost- and environmentally effective strategy across both archetypes is S.01b. This uses bio-based materials and achieves intermediate energy performance. Nevertheless, like other retrofit alternatives, the payback period exceeds 50 years, making this solution unadvisable for homeowners under current energy prices. From an environmental perspective, instead, embodied emissions from retrofit interventions are offset within 14–30 years, depending on scenario and archetype. Achieving large-scale, cost-effective decarbonization of the existing building stock thus requires not only technological optimization but also systemic policy changes. Stronger carbon taxation, improved financial mechanisms, and enhanced workforce training are essential to stimulate market uptake of deep renovations.

Finally, UA revealed that energy price variability most strongly influences GC, causing average increases of up to 48.7% in Archetype A and 39.6% in Archetype B. The electricity mix, climate change, and occupant type most affect wLCE. They cause average variations up to 42.3% in Archetype A and 39.4% in Archetype B, depending on scenario and parameter. Temperature setpoints, materials service life, and quantities strongly impact both indicators. Given the significant variability in the results, UA post-processing revealed scenario S.01a as the most preferred, unlike what emerged from the MOO post-processing. It is therefore essential to incorporate these parameters into decision-making for robust retrofit solutions.

CRediT authorship contribution statement

Aurora Bertini: Writing – review & editing, Writing – original draft, Visualization, Validation, Software, Methodology, Investigation, Data curation, Conceptualization. **Deepak Amaripadath:** Writing – review & editing, Resources. **Emilie Gobbo:** Writing – review & editing, Resources, Methodology, Conceptualization. **Shady Attia:** Writing – review & editing, Writing – original draft, Validation, Supervision, Methodology, Investigation, Formal analysis, Conceptualization.

Declaration of competing interest

The authors declare the following financial interests/personal relationships which may be considered as potential competing interests: Aurora Bertini reports financial support was provided by Fonds de la Recherche Scientifique (FNRS). If there are other authors, they declare that they have no known competing financial interests or personal relationships that could have appeared to influence the work reported in this paper.

Acknowledgement

We gratefully acknowledge the Sustainable Building Design (SBD) Lab at the University of Liège for access to its computational resources, in particular the SCORPION workstation, which enabled the intensive computations required for this study. We also extend our thanks to the IEA Annex 89 – Ways to Implement Net-zero Whole Life Carbon Buildings for the valuable collaborative exchanges and insights. Financial support was provided by the Fonds de la Recherche Scientifique (FNRS) under the PDR project RENOWAVE [T.0004.23F] 2023-2027.

Appendix A

.

Table A1
Energy model inputs for the base cases and each renovation scenario.

	BC A	BC B	S.01a	S.01b	S.01c	S.01d	S.02a	S.02b
Geometry								
Gross floor area [m^2]	235	152	235 (A) 152 (B)		235 (A) 152 (B)		235 (A) 152 (B)	
Occupation density [m^2/p]	129.5	74	129.5 (A) 74 (B)		129.5 (A) 74 (B)		129.5 (A) 74 (B)	
WWR [-]	12%	10%	12% (A) 10% (B)		12% (A) 10% (B)		12% (A) 10% (B)	
Orientation [°]	135	45	135 (A) 45(B)		135 (A) 45(B)		135 (A) 45(B)	
Structure								
Structural type [-]	Load-bearing walls, timber roof beams, cast concrete and hourdi concrete block slabs (A), prefabricated concrete slab (B)							
Envelope								
Infiltration rate [ach]*	0.87	0.83	Min: 0.12, Int: 0.03 Max: 0.30		Min: 0.12, Int: 0.03 Max: 0.30		Min: 0.04, Int: 0.01 Max: 0.09	
External wall U-value [W/(m^{2}K)]	1.72	1.70	Min: 0.80 Int: 0.04 Max: 1.00		Min: 0.80 Int: 0.04 Max: 1.00		Min: 0.15 Int: 0.05 Max: 0.40	
Ground floor U-value [W/(m^{2}K)]	0.46	0.46	0.46		0.46		0.46	
Roof U-value [W/(m^{2}K)]	1.25	1.40	Min: 0.80 Int: 0.04 Max: 1.00		Min: 0.80 Int: 0.04 Max: 1.00		Min: 0.15 Int: 0.05 Max: 0.40	
Insulation material	Trad.	Trad.	Trad.	Biob.	Trad.	Biob.	Trad.	Biob.
Door U-value [W/(m^{2}K)]	2.8	2.8	Min: 1.40 Int: 0.10 Max: 2.00		Min: 1.40 Int: 0.10 Max: 2.00		Min: 0.80 Int: 0.10 Max: 1.20	
Glazing U-value	2.90	2.76	Min: 1.30 Int: 0.10 Max: 1.80		Min: 1.30 Int: 0.10 Max: 1.80		Min: 0.80 Int: 0.10 Max: 1.20	
Glazing g-value	0.74	0.60	Min: 0.40 Int: 0.04 Max: 0.60		Min: 0.40 Int: 0.04 Max: 0.60		Min: 0.20 Int: 0.02 Max: 0.30	
Solar shading	External shade rolls	External shade rolls	External shade rolls		External shade rolls		External shade rolls	
Systems								
Heating generation [-]	Gas boiler	Gas boiler	Reversible heat pump		Reversible heat pump		Reversible heat pump	
Heating generation COP	0.76	0.80	Min: 2.50 Int: 0.25 Max: 3.75		Min: 2.50 Int: 0.25 Max: 3.75		Min: 4.00 Int: 0.25 Max: 5.50	
Delivered hot water temperature [°C]	60	60	55		55		35	
Heating setpoint [°C]	16–23	18–22	16–23 (A) 18–22 (B)		16–23 (A) 18–22 (B)		16–23 (A) 18–22 (B)	
Cooling generation [-]	–	–	Reversible heat pump		Reversible heat pump		Reversible heat pump	
Cooling generation EER	–	–	Min: 3.00 Int: 0.25 Max: 4.25		Min: 3.00 Int: 0.25 Max: 4.25		Min: 4.50 Int: 0.25 Max: 6.00	
Chilled water temperature [°C]	–	–	18		18		18	
Cooling setpoint [°C]	–	–	26		26		26	
Ventilation system [-]	Natural	Natural	Hybrid (system C)		Hybrid (system D)		Hybrid (system D)	
Natural ventilation flow rate [ach]	5	5	5		5		5	
Mechanical ventilation flow rate [l/s/person]	–	–	10		10		10	
Mech. vent. air supply temperature [°C]	–	–	18/26		18/26		18/26	
Heat recovery [-]	–	–	75%		75%		75%	
Lighting power density [W/m2]	8–12	8–12	3		3		1.5	
Lamp type [-]	Fluorescent	Fluorescent	LED		LED		LED	
Equipment power density [W/m^2]	9	9	9		9		9	
PV surface [m^2]	–	–	12		12		32	
PV efficiency [-]	–	–	Min: 0.13 Int: 0.01 Max: 0.16		Min: 0.13 Int: 0.01 Max: 0.16		Min: 0.15 Int: 0.01 Max: 0.20	
Solar thermal surface [m2]	–	–	–		–		5	
Storage								
Water tank volume [m3]	–	–	Min: 0.15 Int: 0.05 Max: 0.30		Min: 0.15 Int: 0.05 Max: 0.30		Min: 0.15 Int: 0.05 Max: 0.30	
Inverter efficiency	–	–	98%		98%		98%	
Battery nominal energy [kWh]	–	–	5		5		10	
Charging current	–	–	5840		5840		5840	
Discharging current	–	–	4000		4000		4000	

* included in the multi-objective optimization

Table A2
Global cost calculation for each renovation scenario.

	BC	S.01a	S.01b	S.01c	S.01d	S.02a	S.02b
Archetype A							
House purchase [€$_{2025}$/m^2]	1270	1270	1270	1270	1270	1270	1270
Finishes RC [€$_{2025}$/m^2]	0	270	280	270	280	295	345
Envelope RC [€$_{2025}$/m^2]	0	475–485	505–525	475–485	505–525	635–730	730–1110
Systems RC [€$_{2025}$/m^2]	0	180–200	180–200	230–250	230–250	355–400	355–400
Storage RC [€$_{2025}$/m^2]	0	25	25	25	25	55	55
Others RC [€$_{2025}$/m^2]	0	140	140	140	140	230	230
Total RC [€$_{2025}$/m^2]	**0**	**1090–1130**	**1130–1170**	**1140–1170**	**1180–1220**	**1570–1710**	**1715–2140**
Project cost [€$_{2025}$/m^2]	0	80–85	85–90	85–90	90–95	120–130	130–160
Maintenance cost [€$_{2025}$/m^2]	70	80–115	80–115	130–165	130–165	170–240	170–240
Actualized replacement cost [€$_{2025}$/m^2]	550	845–865	845–865	1020–1040	1020–1040	1340–1350	1340–1350
Residual value [€$_{2025}$/m^2]	120	200	205	220	225	330	335
Actualized disposal cost [€$_{2025}$/m^2]	5	10	10	10	10	10	15
Energy cost [€$_{2025}$/m^2]	540	275–515	270–500	395–660	405–615	165–210	165–210
CO_2 emissions cost [€$_{2025}$/m^2]	450	100–180	100–180	150–240	150–230	15–65	15–65
GC [€$_{2025}$/m^2]	**2805**	**3630–3890**	**3665–3915**	**4070–4335**	**4110–4340**	**4420–4560**	**4580–5020**
Archetype B							
House purchase [€$_{2025}$/m^2]	1840	1840	1840	1840	1840	1840	1840
Finishes RC [€$_{2025}$/m^2]	0	440	455	440	460	485	555
Envelope RC [€$_{2025}$/m^2]	0	730–750	770–800	730–750	770–800	970–1125	1090–1635
Systems RC [€$_{2025}$/m^2]	0	250–270	250–270	325–350	325–350	475–545	475–545
Storage RC [€$_{2025}$/m^2]	0	40	40	40	40	90	90
Others RC [€$_{2025}$/m^2]	0	215	215	215	215	360	360
Total RC [€$_{2025}$/m^2]	**0**	**1675–1720**	**1730–1780**	**1750–1795**	**1870–1965**	**2380–2605**	**2660–3190**
Project cost [€$_{2025}$/m^2]	0	125–130	135–140	130–135	140–145	175–195	195–270
Maintenance cost [€$_{2025}$/m^2]	120	130–180	130–180	180–220	180–220	255–330	255–330
Actualized replacement cost [€$_{2025}$/m^2]	750	1160–1220	1160–1220	1430–1490	1430–1490	1715–1820	1715–1820
Residual value [€$_{2025}$/m^2]	200	210	215	225	235	320	370
Actualized disposal cost [€$_{2025}$/m^2]	5	15	15	15	15	15	15
Energy cost [€$_{2025}$/m^2]	640	370–600	370–565	550–765	475–630	220–345	220–345
CO_2 emissions cost [€$_{2025}$/m^2]	440	105–185	105–180	165–240	160–235	45–100	45–100
GC [€$_{2025}$/m^2]	**3565**	**5290–5600**	**5345–5630**	**5910–6200**	**5950–6230**	**6505–6750**	**6755–7360**

Table A3
Average annual energy use for each renovation scenario and archetype.

RS	H	C	V	L	E	PV p	PV u	PV s	Tot	Net	O	E	Tot	O%
Archetype A														
BC	149	–	–	14.9		–	–	–	166	166	32	8.5	40.5	79
S.01a	36.0	0.3	3.8	4.8	3.0	1515	1376	139	47.9	40.3	7.5	7.1	14.6	52
S.01b	35.0	0.3	3.8	4.8	3.0	1523	1385	138	47.0	39.4	7.3	6.6	13.9	53
S.01c	36.0	0.6	10.2	4.8	3.0	1518	1446	72	64.8	57.2	10.5	7.2	17.7	59
S.01d	35.1	0.6	10.2	4.8	3.0	1525	1452	72	63.9	56.3	10.3	6.6	16.9	61
S.02a	13.1	0.4	9.0	2.4	3.0	5185	3052	2133	35.7	9.9	2.2	8.5	10.7	20
S.02b	12.8	0.4	9.0	2.4	3.0	5178	3052	2126	35.4	9.6	2.2	8.2	10.4	21
Archetype B														
BC	140	–	–	17.7		–	–	–	158	158	33	12.7	45.7	72
S.01a	33.5	0.2	3.3	2.7	6.7	1461	1393	78	66.5	55.3	10.1	10.7	20.8	46
S.01b	32.7	0.2	3.3	2.7	6.7	1476	1403	83	65.2	53.9	9.9	10.2	20.1	47
S.01c	28.0	1.2	10.8	2.7	6.7	1466	1444	25	88.8	77.5	14.0	11.0	25.0	54
S.01d	27.5	1.2	10.8	2.7	6.7	1470	1448	22	88.0	76.7	13.8	10.3	24.1	55
S.02a	14.8	1.5	9.9	1.3	6.7	4532	3288	1244	61.1	26.3	5.1	14.1	19.2	23
S.02b	14.5	1.5	9.9	1.3	6.7	4545	3291	1253	60.8	25.8	5.0	13.8	18.8	24

RS = Renovation strategy [-] / H = Heating and DHW [kWh/(m$^{2\cdot}$ y)] / C = Cooling [kWh/(m$^{2\cdot}$ y)] / V = Ventilation [kWh/(m$^{2\cdot}$ y)] / L = Lighting [kWh/(m$^{2\cdot}$ y)] / E = Equipment [kWh/(m$^{2\cdot}$ y)] / PV p = PV production [kWh/ y]/ PV u = PV self-use [kWh/ y] / PV s = PV sold [kWh/ y] / Tot = Total energy use intensity [kWh/(m$^{2\cdot}$ y)] / Net = Net energy use intensity [kWh/(m$^{2\cdot}$ y)] / O = Operational emissions [kgCO$_2$e/(m$^{2\cdot}$ y)] / E = Embodied emissions [kgCO$_2$e/(m$^{2\cdot}$ y)] / Tot = Total emissions [kgCO$_2$e/(m$^{2\cdot}$ y)] / O/E = share operational emissions [%].

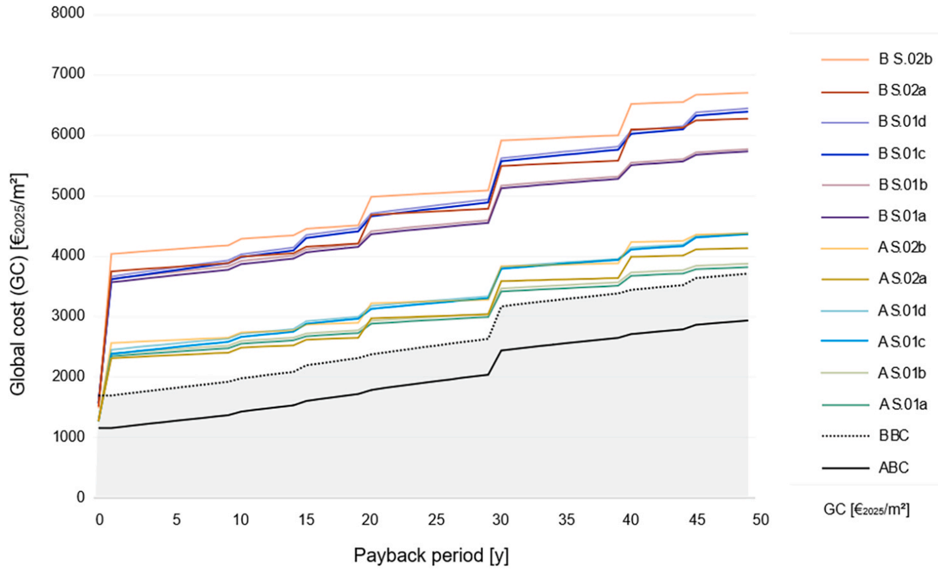

Fig. A.1. Economic payback period including initial subsidies

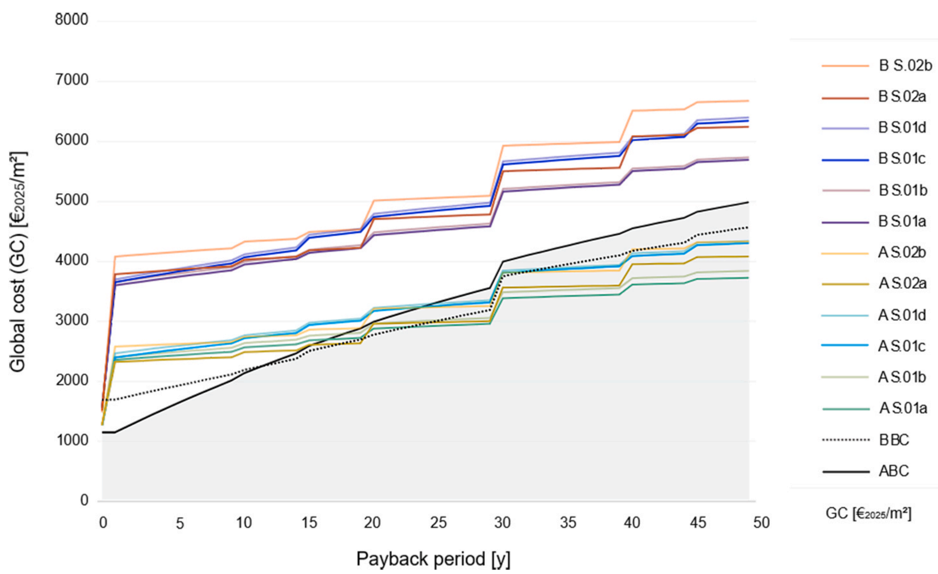

Fig. A.2. Economic payback period including initial subsidies, higher carbon taxation and the inverse gas-to-electricity ratio

Data availability

Data will be made available on request.

References

[1] Y. Al-Kabaha, K. Bataineh, M. Aburabi'e, Multi-objective optimization of energy consumption, cost and emission for a residential building, Heliyon 11 (3) (2025), https://doi.org/10.1016/j.heliyon.2025.e42139.

[2] D. Amaripadath, D.J. Sailor, A. Bertini, M. Barker, S. Attia, Are net zero energy buildings necessarily also net zero emission buildings? Time-integrated analysis using dynamic grid emission factors, Build. Environ. 283 (2025) 113367, https://doi.org/10.1016/j.buildenv.2025.113367.

[3] American Society of Heating, Refrigerating and Air-Conditioning Engineers (ASHRAE). (2022). *Energy Standard for Sites and Buildings Except Low-Rise Residential Buildings* (Standard 90.1-2022). ASHRAE, Atlanta, GA, USA. https://www.ashrae.org/technical-resources/bookstore/standard-90-1.

[4] Association Belge des Experts (ABEX). (2023). *Bordereau ABEX pour la construction privée.*

[5] S. Attia, A. Mustafa, N. Giry, M. Popineau, M. Cuchet, N. Gulirmak, Developing two benchmark models for post-world war II residential buildings, Energ. Buildings 244 (2021) 111052, https://doi.org/10.1016/j.enbuild.2021.111052.

[6] S. Attia, S. Petersen, E. Hoxha, E. Gobbo, A. Bertini, M. Dasse, H. Abu-Ghaida, M. Heiranipour, M. Al-Obaidy, A. Norouziasas, & A. Stephan (2024). *Framework to Model Building Carbon Emissions. (Version 5).* Liege, Belgium: Sustainable Building Design Lab. https://doi.org/10.13140/RG.2.2.15338.73925/4. https://orbi.uliege.be/handle/2268/316958.

[7] A. Bertini, M. Al-Obaidy, M. Dasse, D. Amaripadath, E. Gobbo, S. Attia, Parametrization of variables affecting the whole life carbon performance of nearly zero energy residential building renovation, Build. Environ. 278 (2025) 113013, https://doi.org/10.1016/j.buildenv.2025.113013.

[8] A. Bertini, H. Lamy, A. Norouziasas, D. Van Dijk, A. Dama, S. Attia, Control algorithm for dynamic solar shadings: a simulation study for office buildings based on ISO 52016-3, Build. Environ. 262 (2024) 111818, https://doi.org/10.1016/j.buildenv.2024.111818.

[9] Brinkhaus, M. (2025). *EU Energy Outlook 2060—Europe's energy future through 2060.* Montel AS. Oslo, Norway. https://tinyurl.com/yckxzx4j.

[10] S. Carbonelle, S. Nourricier, S. Monfils, J. Lambert, I. Nijskens, P. Bruge, *COZEB 3—Mise à jour et extension de l'étude CO-ZEB déterminant le niveau de performance*

énergétique optimal en fonction des couts conformément à la Directive 2010/31/EU et analyse de sensibilité des résultats obtenus, Belgium (2023).

[11] CEN. (2011). EN 15978: Sustainability of construction works—Assessment of environmental performance of buildings—Calculation method. European Committee for Standardization, Brussels, Belgium.

[12] CEN. (2015). EN 16627:2015—Sustainability of construction works—Assessment of economic performance of buildings—Calculation methods. European Committee for Standardization, Brussels, Belgium.

[13] CEN. (2017). EN 15459-1:2017—Energy performance of buildings—Economic evaluation procedure for energy systems in buildings—Part 1: Calculation procedures, Module M1-14. European Committee for Standardization, Brussels, Belgium.

[14] CEN. (2019). EN 15804+A2: Sustainability of construction works—Environmental product declarations—Core rules for the product category of construction products. European Committee for Standardization, Brussels, Belgium.

[15] Chartered Institution of Building Services Engineers (CIBSE). (2024). *TM65 Embodied carbon in building services: A calculation methodology*. London, UK.

[16] Climate Action Network Europe. (2025). *National Building Renovations Plans (NBRP): A Powerful tool for a just and climate-resilient built environment*. https://caneurope.org/content/uploads/2025/06/Briefing-National-Building-Renovations-Plans.pdf.

[17] DareToCompare.be. (2025). *kWh feed-in rates*. https://www.daretocompare.be/energy/feed-in.

[18] K. Deb, A. Pratap, S. Agarwal, T. Meyarivan, A fast and elitist multiobjective genetic algorithm: NSGA-II, IEEE Trans. Evol. Comput. 6 (2) (2002) 182–197, https://doi.org/10.1109/4235.996017.

[19] Y. Decorte, N. Van Den Bossche, M. Steeman, Guidelines for defining the reference study period and system boundaries in comparative LCA of building renovation and reconstruction, Int. J. Life Cycle Assess. 28 (2) (2023) 111–130, https://doi.org/10.1007/s11367-022-02114-0.

[20] F. Dehghan, C. Porras Amores, Simulation-based Multi-Objective Optimization for Building Retrofits in Iran: addressing Energy Consumption, Emissions, Comfort, and Indoor Air Quality considering climate Change, Sustainability 17 (5) (2025) 2056, https://doi.org/10.3390/su17052056.

[21] DesignBuilder. (2024). *DesignBuilder* (Version 7.3.0) [Software]. https://designbuilder.co.uk/.

[22] Electricity Maps. (2024). https://www.electricitymaps.com/.

[23] *Energy Performance of Buildings Directive*. (2024). https://energy.ec.europa.eu/topics/energy-efficiency/energy-performance-buildings/energy-performance-buildings-directive_en.

[24] *Energy renovation: European ambition built on structured support*. (2025). BNP Paribas. https://group.bnpparibas/en/news/energy-renovation-european-ambition-built-on-structured-support.

[25] European Commission. (2021). *European Climate Law—Climate Action*. https://climate.ec.europa.eu/eu-action/european-climate-law_en.

[26] European Commission. (2024). *Heat Pumps*. https://energy.ec.europa.eu/topics/energy-efficiency/heat-pumps_en.

[27] European Parliament and Council of the European Union. (2024). Directive (EU) 2024/1275 of the European Parliament and of the Council of 24 April 2024 on the energy performance of buildings (recast) (EU 2024/1275). Official Journal of the European Union. http://data.europa.eu/eli/dir/2024/1275/oj.

[28] L. Felicioni, L. Casalone, L. Marchi, J. Gaspari, Integrating life cycle assessment and cost analysis in decision making: Optimising design choices in a public building case study, Energ. Buildings 347 (2025) 116399, https://doi.org/10.1016/j.enbuild.2025.116399.

[29] Gouvernement wallon. (2014). *Annexe A1—Méthode PER - Méthode de détermination du niveau de consommation d'énergie primaire des bâtiments résidentiels*. https://energie.wallonie.be/servlet/Repository/agw-150514-annexe-a1-methode-per-fr.pdf?ID=32297.

[30] C.J. Hopfe, J.L.M. Hensen, Uncertainty analysis in building performance simulation for design support, Energ. Buildings 43 (10) (2011) 2798–2805, https://doi.org/10.1016/j.enbuild.2011.06.034.

[31] International Organization for Standardization (ISO). (2017). *Buildings and constructed assets—Service life planning—Part 5: Life-cycle costing* (ISO 15686-5: 2017). Geneva, Switzerland. https://www.iso.org/standard/61148.html.

[32] International Organization for Standardization (ISO). (2018a). Energy performance of buildings—Overall energy performance assessment procedures Part 2: Guideline for using indoor environmental input parameters for the design and assessment of energy performance of buildings (ISO/TR 17772-2:2018). Geneva, Switzerland. https://www.iso.org/standard/68228.html.

[33] International Organization for Standardization (ISO). (2018b). Energy performance of buildings—Schedule and condition of building, zone and space usage for energy calculation Part 2: Residential buildings (ISO 18523-2:2018). Geneva, Switzerland. https://www.iso.org/standard/69633.html.

[34] M. Jakob, C. Stettler, Netto-Null Treibhausgasemissionen im Gebäudebereich—Methodische Fragen (2023). https://doi.org/10.13140/RG.2.2.12424.19201.

[35] I. Jankovic, S. Zuhaib, X.F. Álvarez, M. Fabbri, H. Sibileau, O. Rapf, Milne, in: *Introducing the Heat Pump Readiness Indicator: How to make Energy Performance Certificates fit for heat pumps*, BEUC, The European Consumer Organisation, 2023.

[36] Z. Khorasani Zadeh, M. Ouf, B. Gunay, B. Delcroix, G. Larochelle Martin, Developing an adaptive thermostat control algorithm for occupant-centric demand response in residential buildings, Energ. Buildings 357 (2026) 117114, https://doi.org/10.1016/j.enbuild.2026.117114.

[37] Kraken Immo. (2025). *Guide complet: Combien coûte une rénovation en Belgique en 2025?* https://www.krakenimmo.com/blog/combien-coute-une-renovation.

[38] C. Leveau, M. Cherdon, M. Vismara, B. Huberlant, *COZEB 2—Détermination du niveau de performance énergétique optimal des bâtiments en fonction des coûts*, Belgium (2017).

[39] L. Luo, H. Wei, Z. Lin, J. Wu, W. Wang, Y. Sun, Multi-objective optimal energy-efficient retrofit determination using hybrid urban building energy model: considering uncertainties between models, Build. Simul. 18 (1) (2025) 183–206, https://doi.org/10.1007/s12273-024-1206-6.

[40] H. Ma, Y. Zhang, S. Sun, T. Liu, Y. Shan, A comprehensive survey on NSGA-II for multi-objective optimization and applications, Artif. Intell. Rev. 56 (12) (2023) 15217–15270, https://doi.org/10.1007/s10462-023-10526-z.

[41] Macrotrends. (n.d.). *Belgium Inflation Rate (1960-2024)*. Retrieved October 9, 2025, from https://www.macrotrends.net/global-metrics/countries/bel/belgium/inflation-rate-cpi.

[42] S. Marino, I.B. Hogue, C.J. Ray, D.E. Kirschner, A Methodology for performing Global uncertainty and Sensitivity Analysis In Systems Biology, J. Theor. Biol. 254 (1) (2008) 178–196, https://doi.org/10.1016/j.jtbi.2008.04.011.

[43] N. Marlair, Quel est le prix d'une rénovation de maison ? TrustUp Blog. (2024). https://blog.trustup.be/fr/prix-renovation-maison/.

[44] Meteonorm. (2024). *Meteonorm* (Version 8) [Software]. https://meteonorm.com/en/meteonorm-version-8.

[45] A.V. Olympios, P. Hoseinpoori, C.N. Markides, Toward optimal designs of domestic air-to-water heat pumps for a net-zero carbon energy system in the UK, Cell Reports Sustainability 1 (2) (2024) 100021, https://doi.org/10.1016/j.crsus.2024.100021.

[46] Passive House Institute. (2023). *Criteria for Buildings. Passive House—EnerPHit—PHI Low Energy Building* (Version 10c). Darmstadt, Germany. https://passiv.de/downloads/03_building_criteria_en.pdf.

[47] S. Petchrompo, D.W. Coit, A. Brintrup, A. Wannakrairot, A.K. Parlikad, A review of Pareto pruning methods for multi-objective optimization, Comput. Ind. Eng. 167 (2022) 108022, https://doi.org/10.1016/j.cie.2022.108022.

[48] Quelle energie. (n.d.). *Quel est le prix d'une rénovation au m² en 2025 ?* Retrieved October 9, 2025, from https://www.quelleenergie.fr/economies-energie/eco-travaux/renovation-globale/prix-m2.

[49] D. Ramon, K. Allacker, Integrating long term temporal changes in the Belgian electricity mix in environmental attributional life cycle assessment of buildings, J. Clean. Prod. 297 (2021) 126624, https://doi.org/10.1016/j.jclepro.2021.126624.

[50] Regione Lombardia. (2024). *Prezzario regionale dei lavori pubblici*. https://www.regione.lombardia.it/wps/portal/istituzionale/HP/DettaglioServizio/servizi-e-informazioni/Enti-e-Operatori/Autonomie-locali/Acquisti-e-contratti-pubblici/Osservatorio-regionale-contratti-pubblici/prezzario-opere-pubbliche/prezzario-opere-pubbliche.

[51] *Renovation wave*. (2020). https://energy.ec.europa.eu/topics/energy-efficiency/energy-performance-buildings/renovation-wave_en.

[52] M. Röck, M.R.M. Saade, M. Balouktsi, F.N. Rasmussen, H. Birgisdottir, R. Frischknecht, G. Habert, T. Lützkendorf, A. Passer, Embodied GHG emissions of buildings – the hidden challenge for effective climate change mitigation, Appl. Energy 258 (2020) 114107, https://doi.org/10.1016/j.apenergy.2019.114107.

[53] G. Ruellan, S. Attia, G. Haesbroeck, Clustering of archetypal building-inhabitant pairs to improve energy efficiency: the case of the Walloon region in Belgium, Energ. Buildings 335 (2025) 115549, https://doi.org/10.1016/j.enbuild.2025.115549.

[54] R. Shan, W. Lai, H. Tang, X. Leng, W. Gu, Residential Building Renovation considering Energy, Carbon Emissions, and cost: an Approach Integrating Machine Learning and Evolutionary Generation, Appl. Sci. 15 (4) (2025) 1830, https://doi.org/10.3390/app15041830.

[55] S.S. Shanbhag, M.K. Dixit, The Impact of Climate Change and Evolving Energy Economy on Key Parameters of the Life Cycle Assessment and Energy Modeling of Buildings. (2023), https://doi.org/10.2139/ssrn.4653289.

[56] Southface Institute. (2016). *Fostering Occupant Engagement for Resource Efficiency*. https://www.southface.org/resource/fostering-occupant-engagement-for-resource-efficiency/.

[57] M. Stein, Large Sample Properties of Simulations using Latin Hypercube Sampling, Technometrics 29 (2) (1987) 143–151, https://doi.org/10.1080/00401706.1987.10488205.

[58] H.A. Taboada, F. Baheranwala, D.W. Coit, N. Wattanapongsakorn, Practical solutions for multi-objective optimization: an application to system reliability design problems, Reliability Engineering & System Safety, Selected Papers Presented at the Fourth International Conference on Quality and Reliability 92 (3) (2007) 314–322, https://doi.org/10.1016/j.ress.2006.04.014.

[59] H. Taboada, D.W. Coit, Post-Pareto optimality analysis to efficiently identify promising solutions for multi-objective problems, Rutgers University ISE Working Paper (2005) 05–15.

[60] TOTEM. (2024). *TOTEM* (Version 3.2.2) [Software]. https://www.totem-building.be/.

[61] J. van Hoof, L. Schellen, V. Soebarto, J.K.W. Wong, J.K. Kazak, Ten questions concerning thermal comfort and ageing, Build. Environ. 120 (2017) 123–133, https://doi.org/10.1016/j.buildenv.2017.05.008.

[62] E.K. Velten, C. Calipel, A. Cornaggia, M. Duwe, N. Evans, C. Felthoefer, J. Gardiner, M. Hagemann, F. Hossfeld, C. Humphreys, L. Kahlen, S. Lalieu, M. Moisio, N. Pelekh, P. Schoeberlein, A. Sniegocki, A. Stefanczyk, J. Tarpey, Wojtylo (2025). https://climateobservatory.eu/report/2025-report-state-eu-progress-climate-neutrality.

[63] S. Wen, R. You, Q. Chen, Implementing building retrofitting strategies to halve campus office building carbon emissions by 2035: a case study in Hong Kong with

techno-economic analysis, Energ. Buildings 338 (2025) 115705, https://doi.org/10.1016/j.enbuild.2025.115705.

[64] G. Wernet, C. Bauer, B. Steubing, J. Reinhard, E. Moreno-Ruiz, B. Weidema, *The ecoinvent database version 3 (part I): Overview and methodology*, Int. J. Life Cycle Assess. 21 (9) (2016) 1218–1230.

[65] M.K. Wiik, A systematic literature review of GHG emission declarations, limit values, and roadmaps for the decarbonisation of buildings, Sustainable Futures 10 (2025) 100846, https://doi.org/10.1016/j.sftr.2025.100846.

[66] X. Zhan, W. Zhang, R. Chen, Y. Bai, J. Wang, G. Deng, Non-dominated sorting genetic algorithm-II: a multi-objective optimization method for building renovations with half-life cycle and economic costs, Build. Environ. 267 (2025) 112155, https://doi.org/10.1016/j.buildenv.2024.112155.

[67] H. Zhang, K. Hewage, E. Bakhtavar, Q. Sun, R. Sadiq, Robust building energy retrofit evaluation under uncertainty: an interpretable machine learning approach, Energ. Conver. Manage. 345 (2025) 120362, https://doi.org/10.1016/j.enconman.2025.120362.

[68] Y. Zhang (n.d.). *jEplus+EA* (Version 2) [Software]. Retrieved November 15, 2024, from https://www.jeplus.org/wiki/doku.php?id=docs:jeplus_ea_v2.